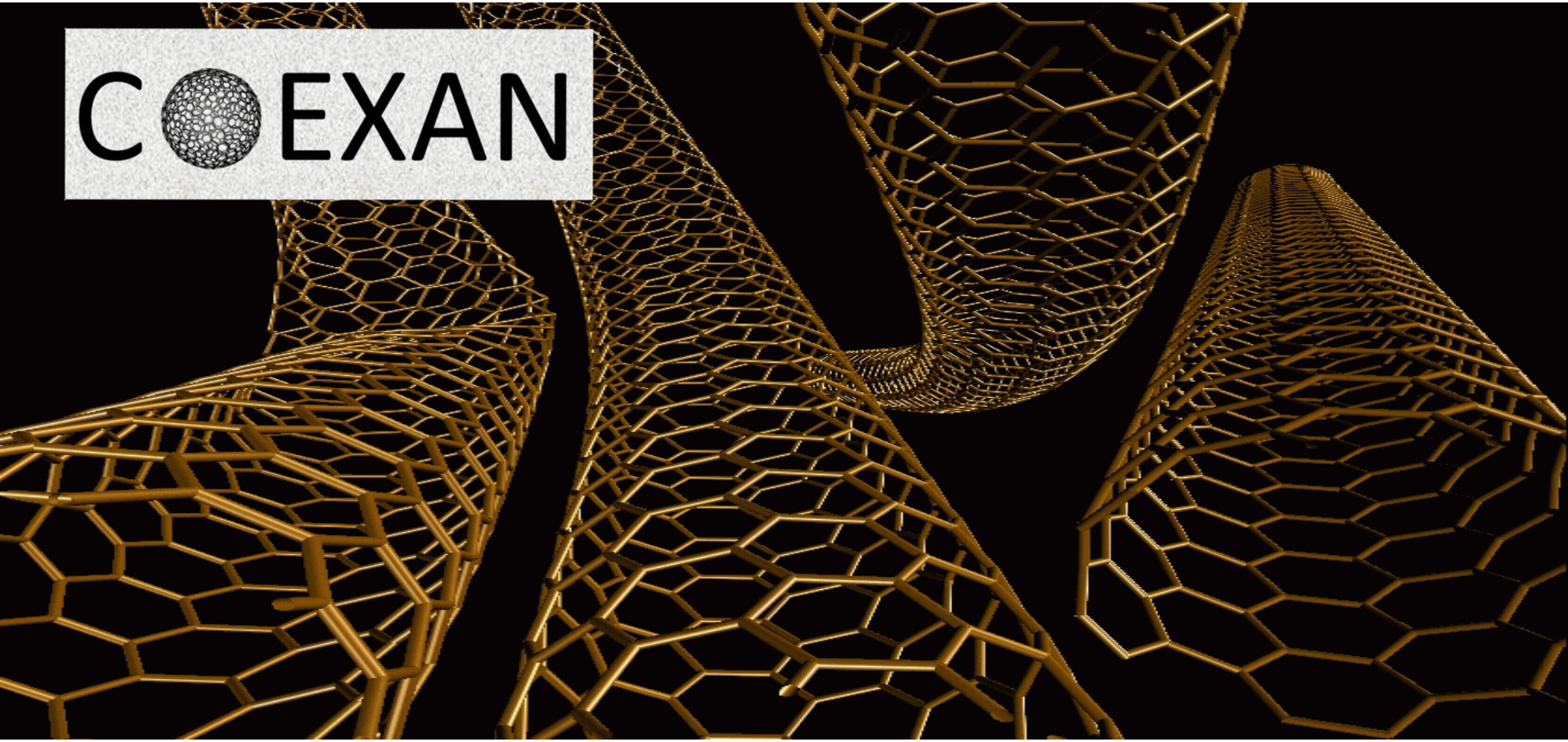

Maurizio De Crescenzi

Dipartimento di Fisica, Universitá di Roma "Tor Vergata", Roma, Italy

decrescenzi@roma2.infn.it

Carbon nanotubes and carbon nanostructures for photovoltaics devices

Solar cells can be classified into various types:

- first generation solar cells made from bulk crystalline Silicon or GaAs;

- second generation solar cells-also called thin film solar cells-
are mainly based on amorphous silicon, cadmium telluride (CdTe), copper indium gallium diselenide (CIGS), or CIS;

- third generation solar cells include dye-sensitized
(Graetzel cells), organic, and nanocrystalline (nanotube, nanowire, nanodots) solar cells.

Renewable energy from the available resources:

- **hydroelectric resource (0.5 TW)**
- **from all tides & ocean currents (2 TW)**
- **geothermal integrated over all of the land area (12 TW)**
- **globally extractable wind power (2-4 TW)**
- **solar energy striking the earth (120,000 TW)**

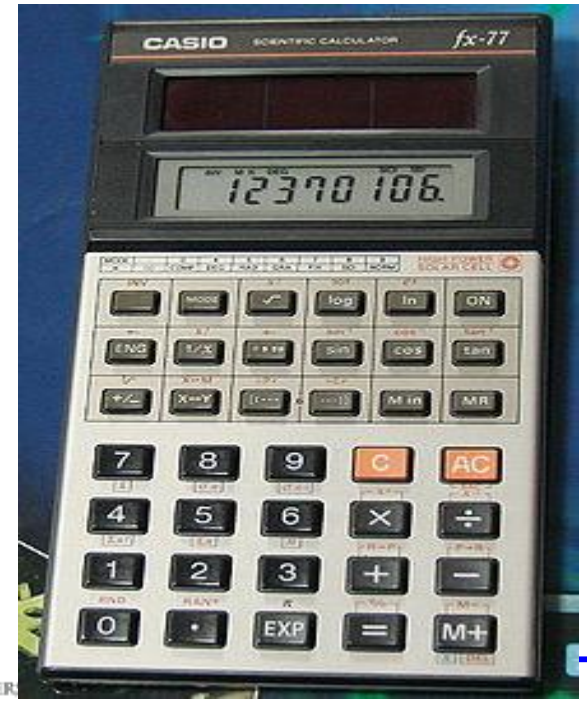

Silicon Solar Cells

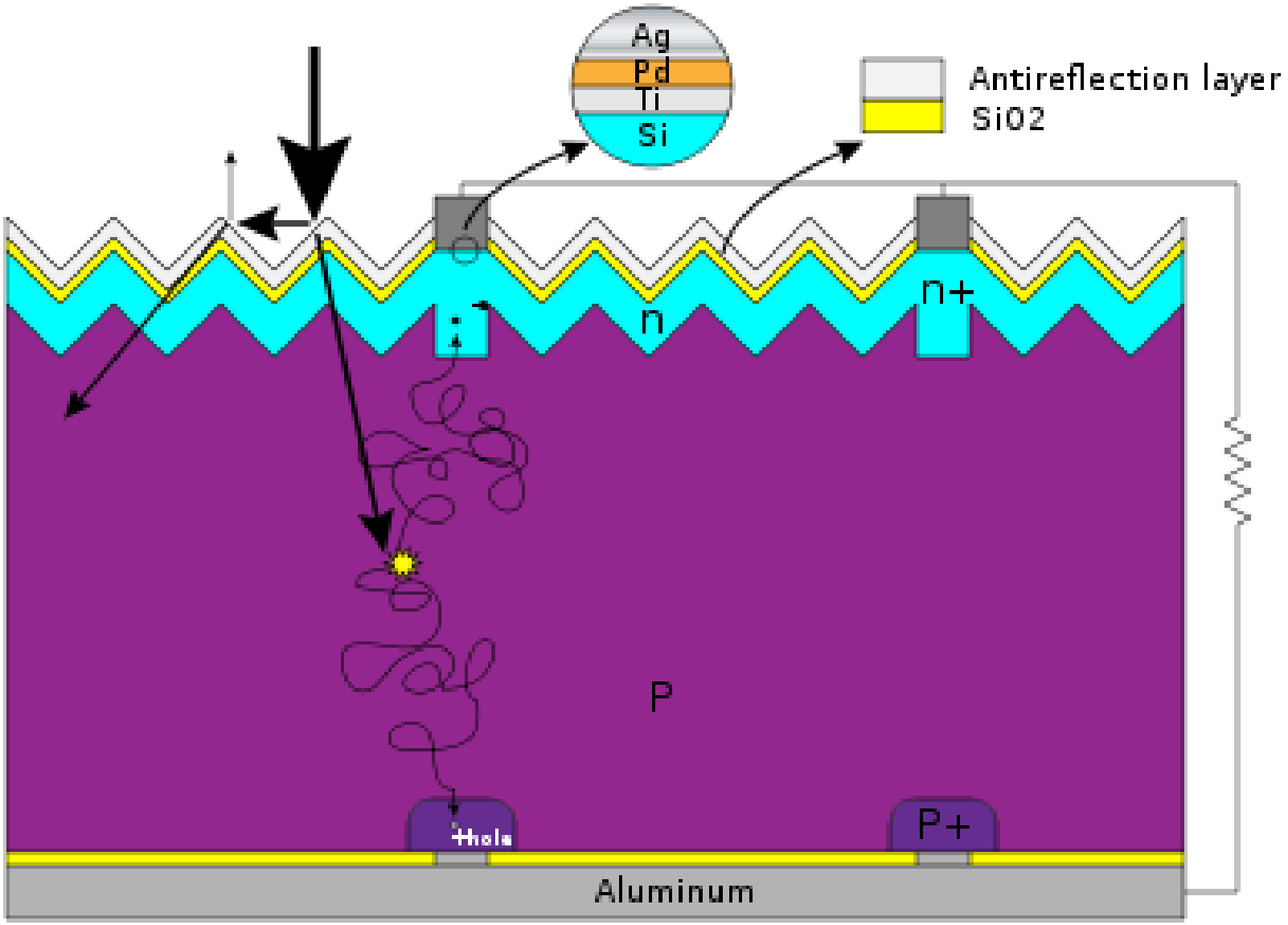
Ag
Pd
Ti
Si
Antireflection layer
SiO2
i
n
n+
P
Hole
P+
Aluminum

Main parameters of a solar cell

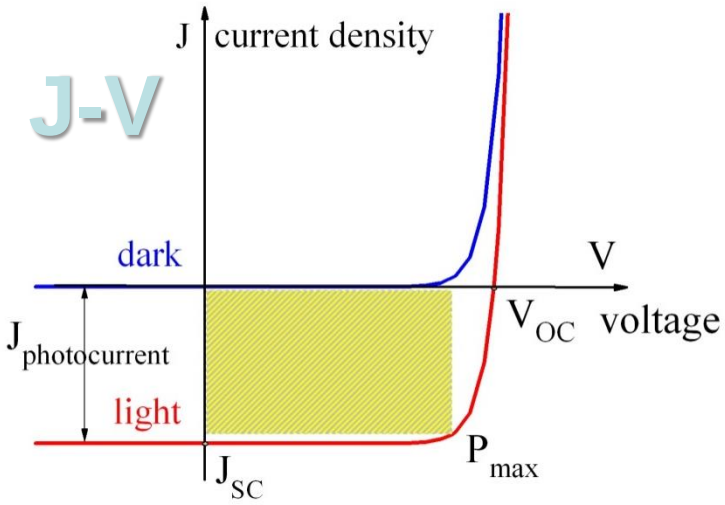

$$FF = 100\,\frac{P_{max}}{J_{sc}V_{oc}}$$

$$PCE = FF\,\frac{J_{sc}V_{oc}}{P_{in}} = \frac{P_{max}}{P_{in}}$$

They are a measure of the cell quality and of the efficiency

$$J = J_0\left(e^{\frac{q(V-JR_s)}{nKT}} - 1\right) + \frac{V - JR_s}{R_p}$$

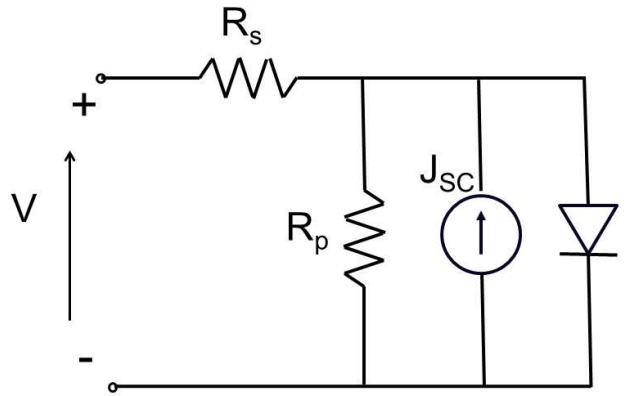

Main parameters of a solar cell

$$EQE(\lambda) = 100\,\frac{hc\,J_{sc}(\lambda)}{e\,\lambda\,P_{in}(\lambda)}$$

Probability for one incident photon of wavelength λ (or energy *E*) to deliver an electron to the external circuit

- **Optical absorption properties**
- **Optoelectronic characteristics of the cell**

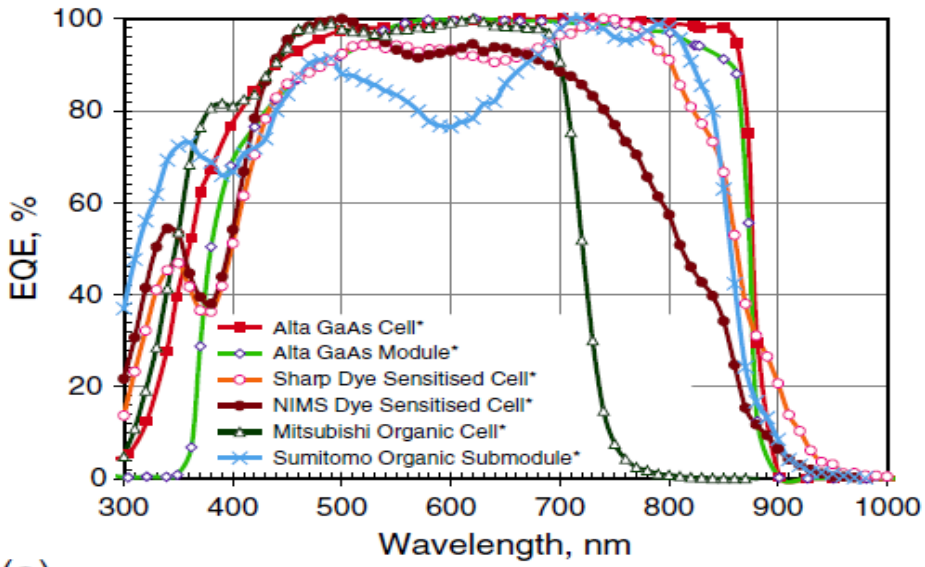

(a)

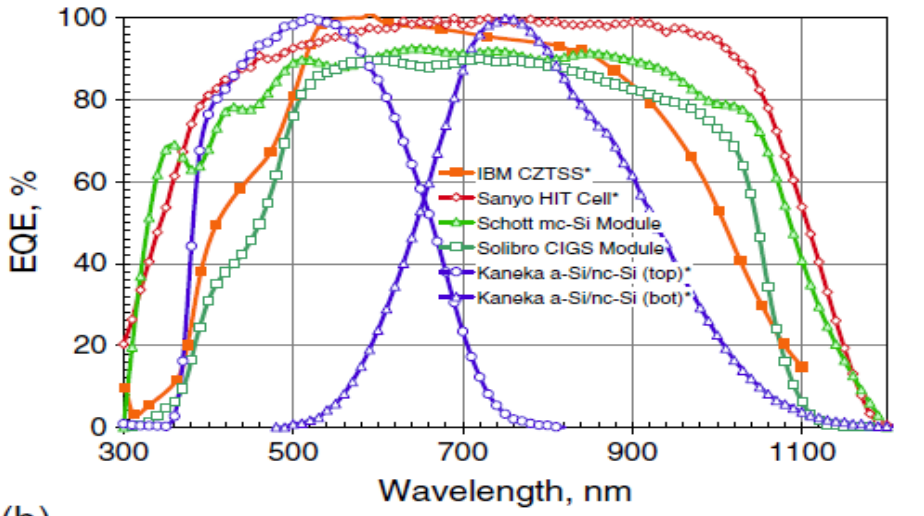

(b)

M. A. Green et al., Prog. Photovolt: Res. Appl. 20, 12–20 (2012)

Outline

-Hystory of the photoconductivity with CNTs

-Methods of Synthesis CVD, Characterization, Devices
-New routes for dispersing CNT on any surface
-CNT/Silicon hybrid solar cell (both SW and MW) with more than 10% efficiency

-Results on MWCNTs and SWCNTs electrochemical (Graetzel) solar cells, decoration with Cu, Au and Ag nanoparticles to enhance the IPCE (%) up to 15%

Various types of nanotubes

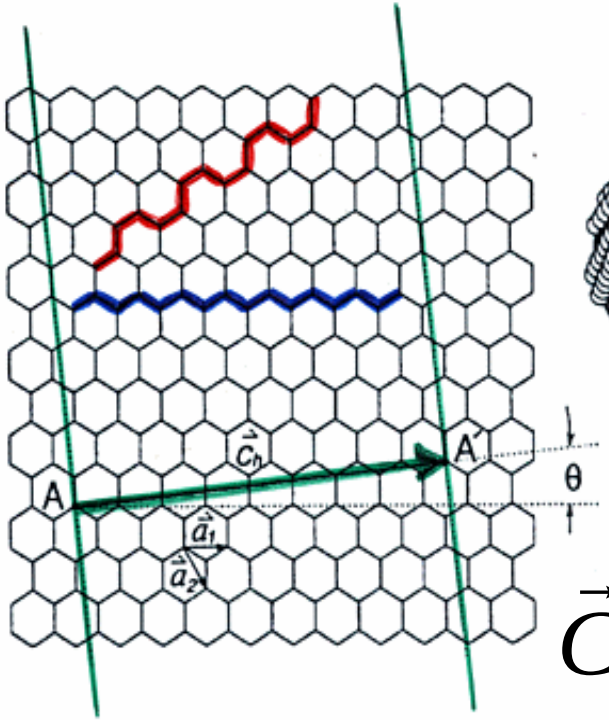

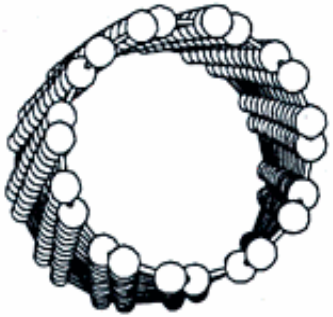

$$\vec{C} = m\vec{a}_1 + n\vec{a}_2$$

'zigzag'

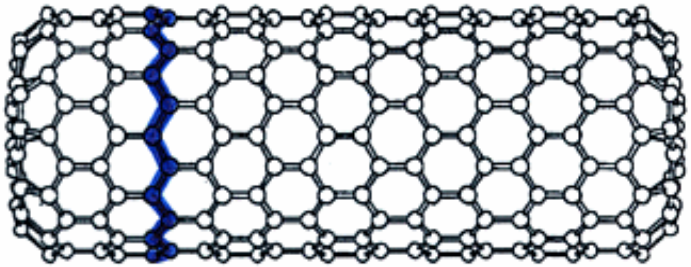

'armchair'

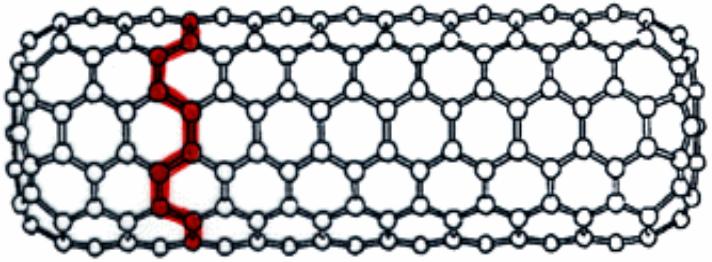

large variety of chiral angles

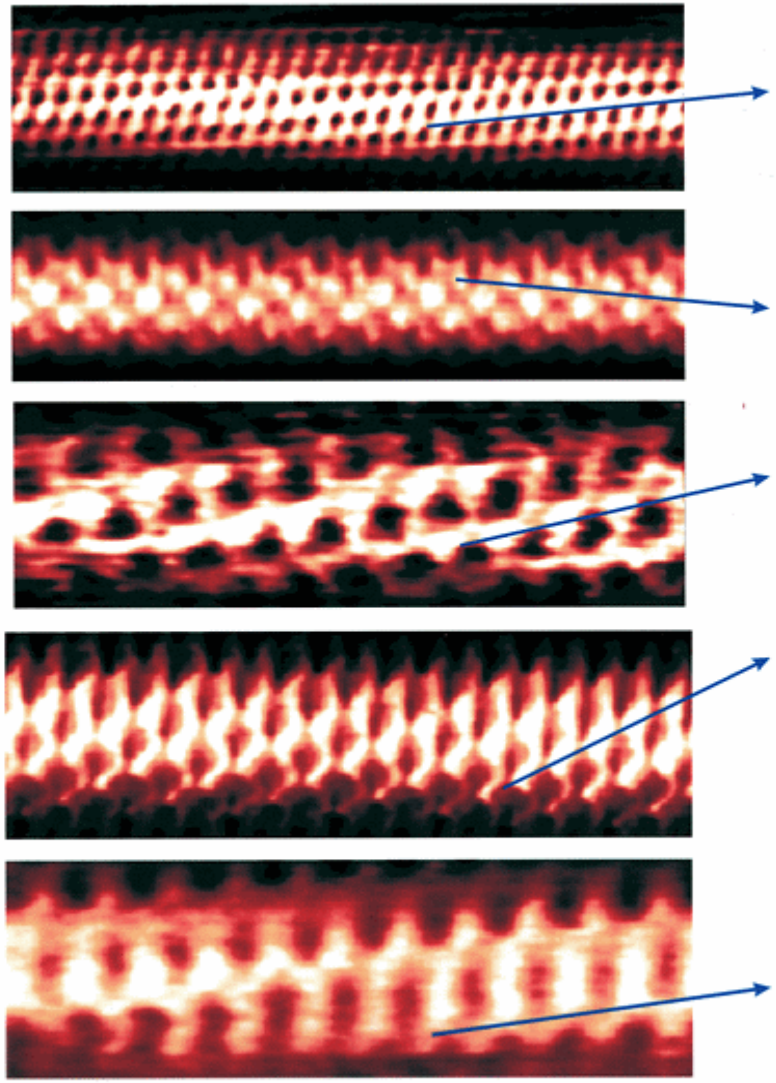

Tube axis

STM images

METAL OR SEMICONDUCTOR ?

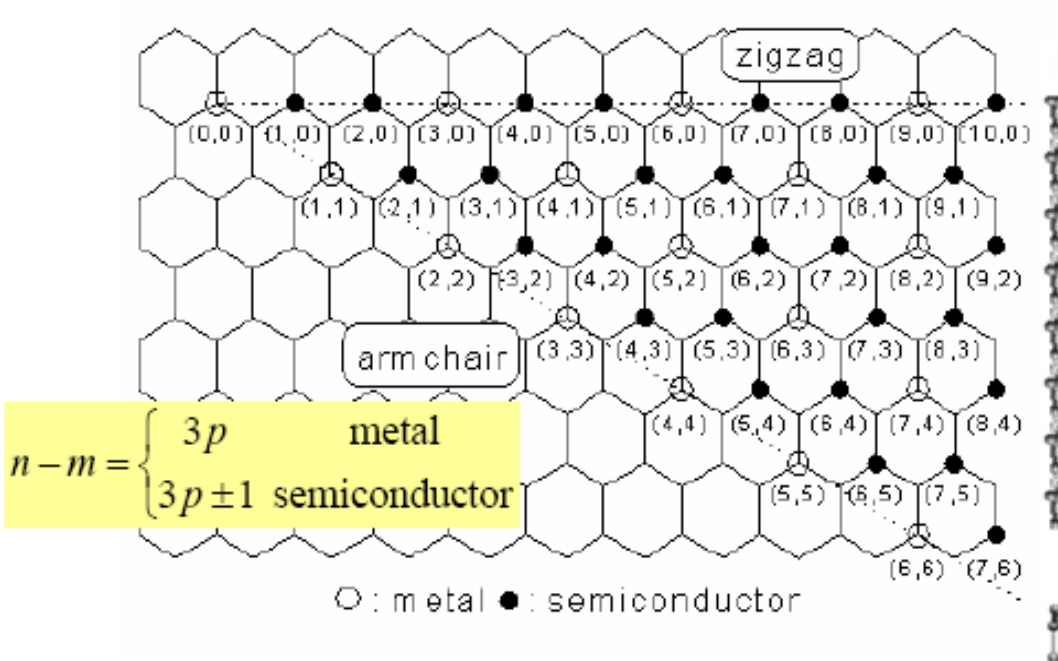

$$n-m=\begin{cases} 3p & \text{metal} \\ 3p\pm1 & \text{semiconductor} \end{cases}$$

a)

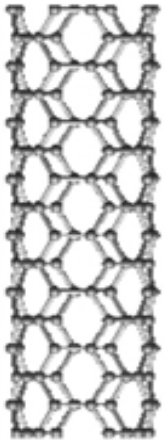

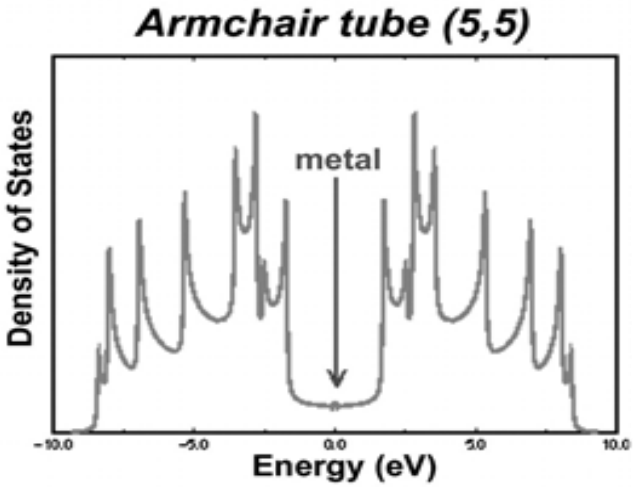

b)

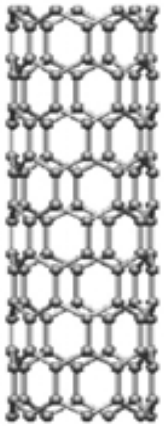

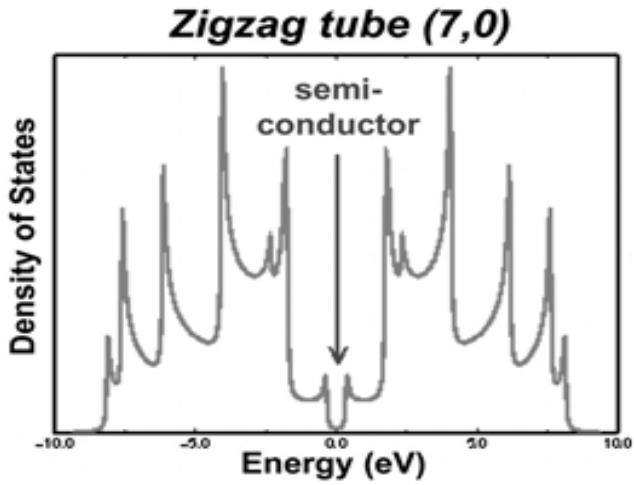

The energy band gap depends on diameter and helicity spacing and varies from less than 0.1 eV to more than 2 eV depending on nanotube diameter.

Carbon Nanotubes (CNT) as building blocks for solar energy conversion devices

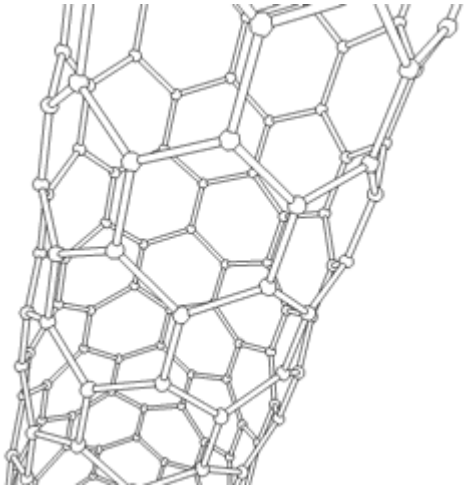

- ✓Unique opto-electronic properties
- ✓Wide stability to oxidation
- ✓High surface area
- ✓Cylindrical morphology provides reactive edges to chemical functionalization and surface modification
- ✓Carbon nanotubes have a band-gap in the range of 0-1.1 eV depending on their chirality and diameter
- ✓No need of selective doping to form p-n junctions

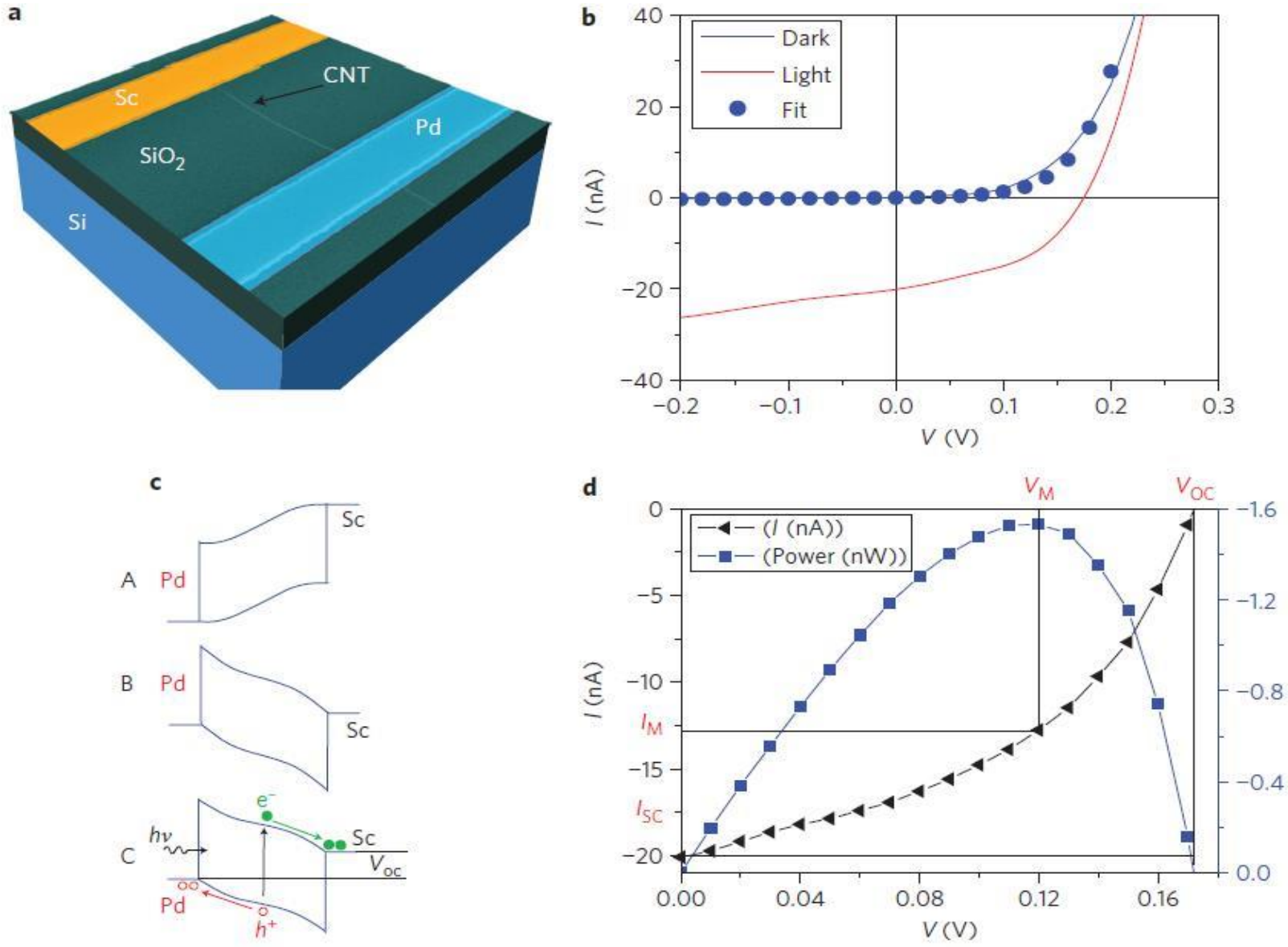

L.Yang et al., Nature Photonics 5, 672 (2011)

- Temperature of the substrate
- Time of exposure
- C_2H_2 pressure

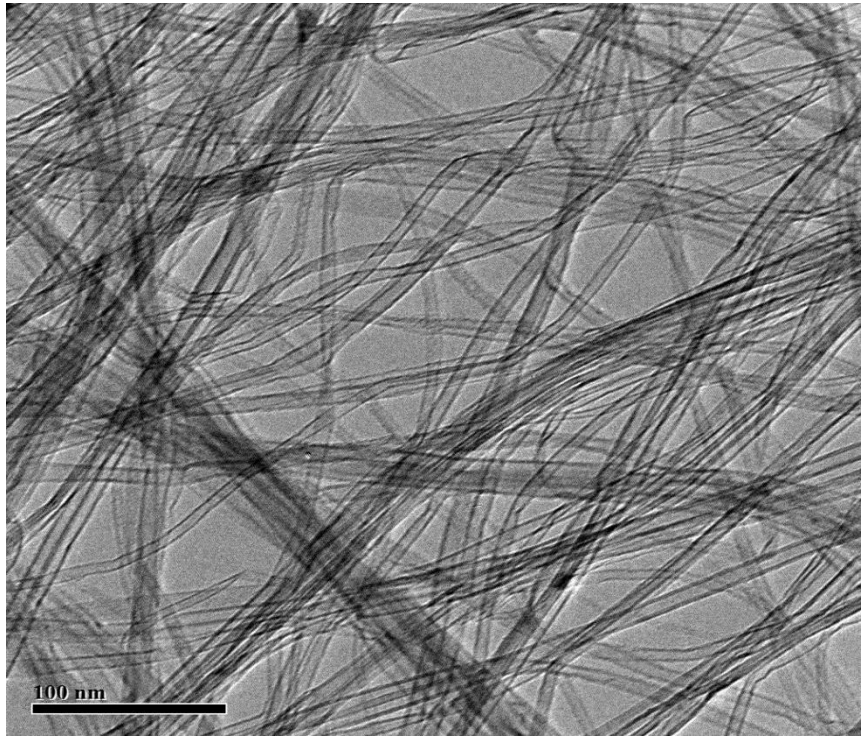

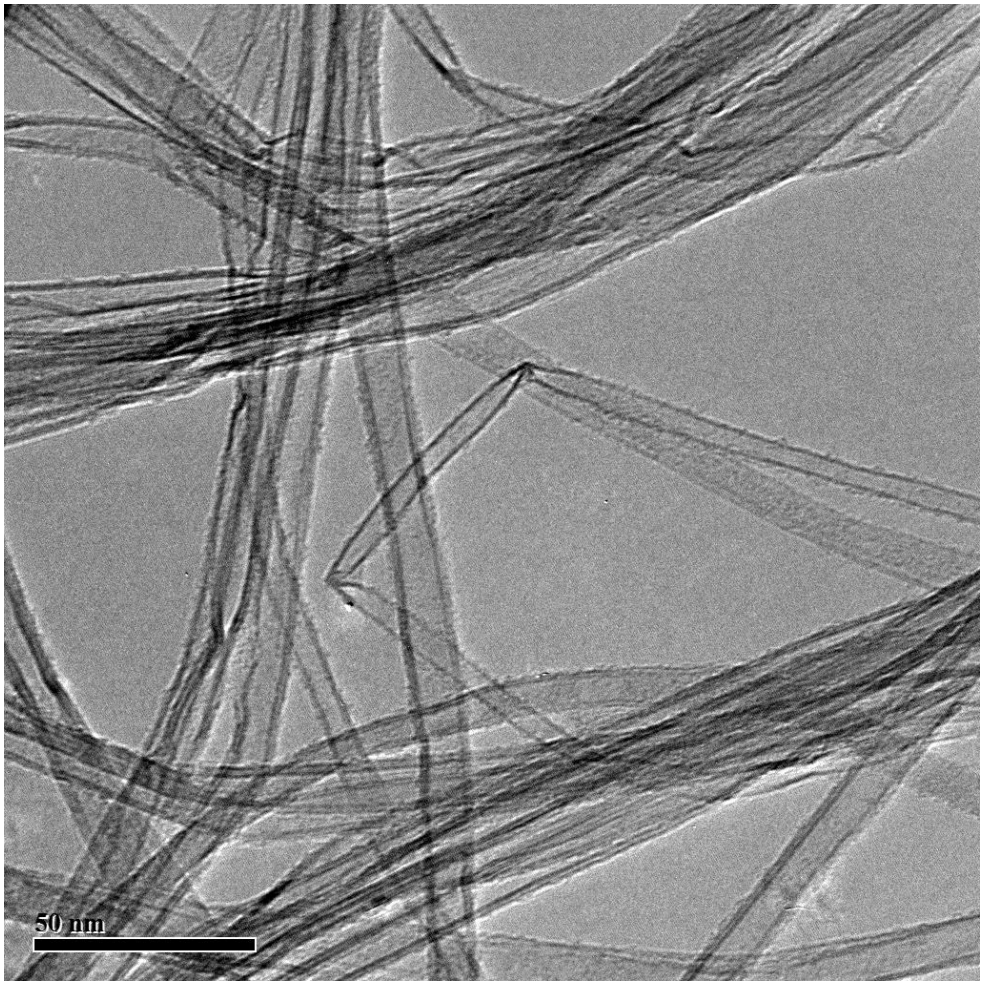

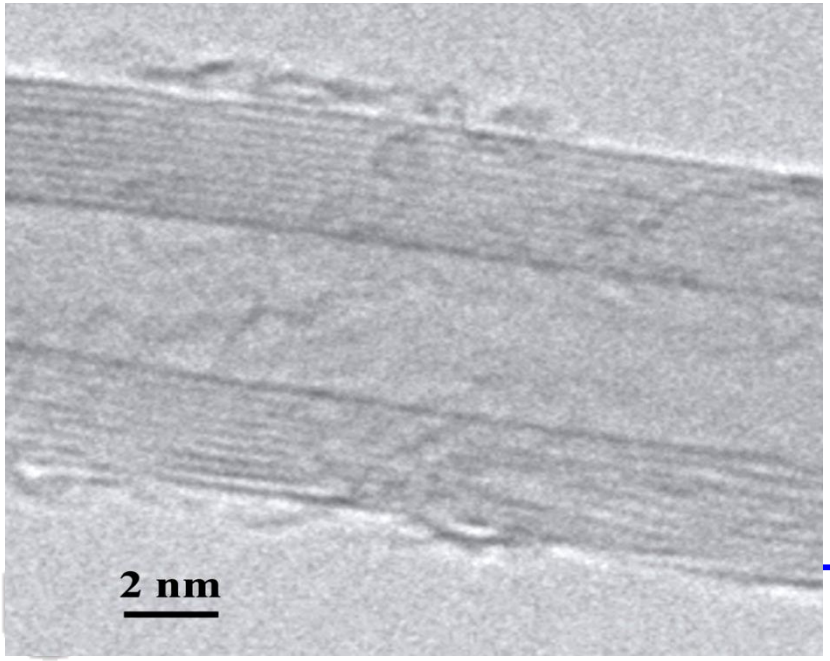

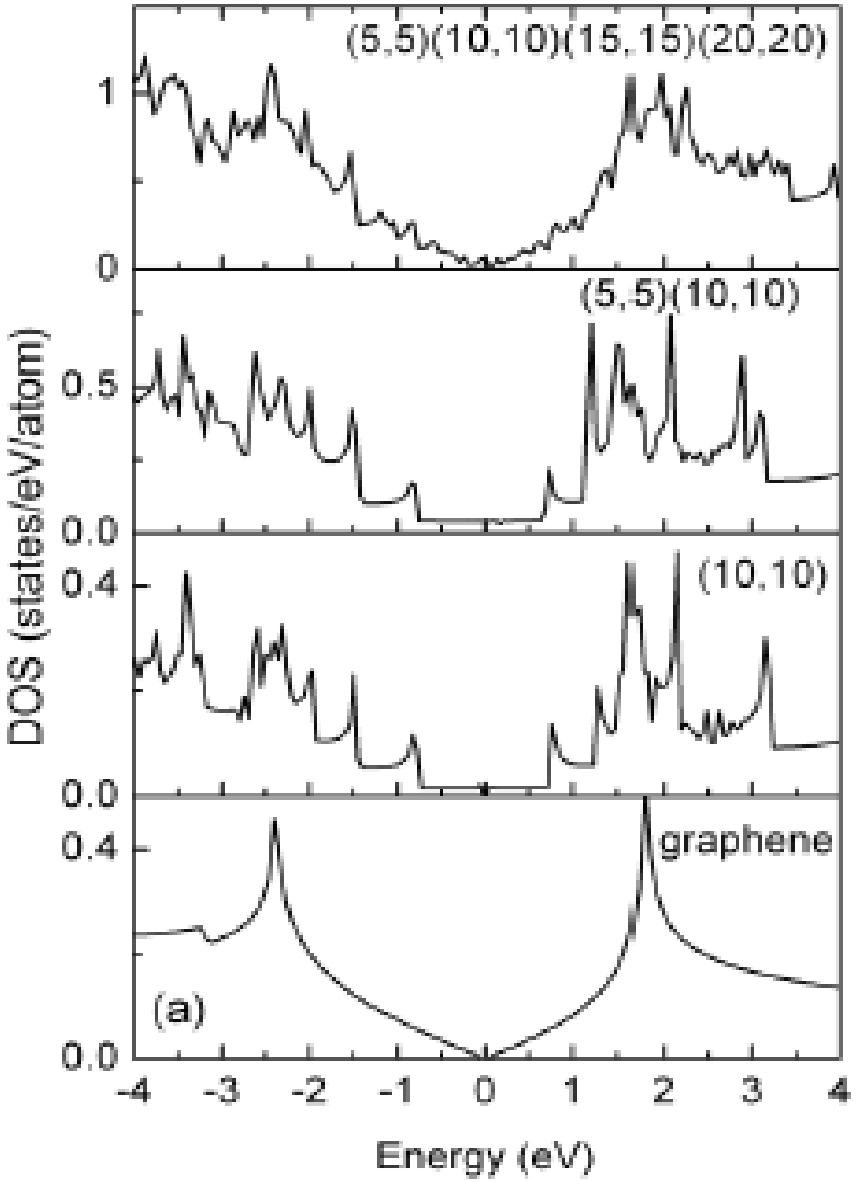

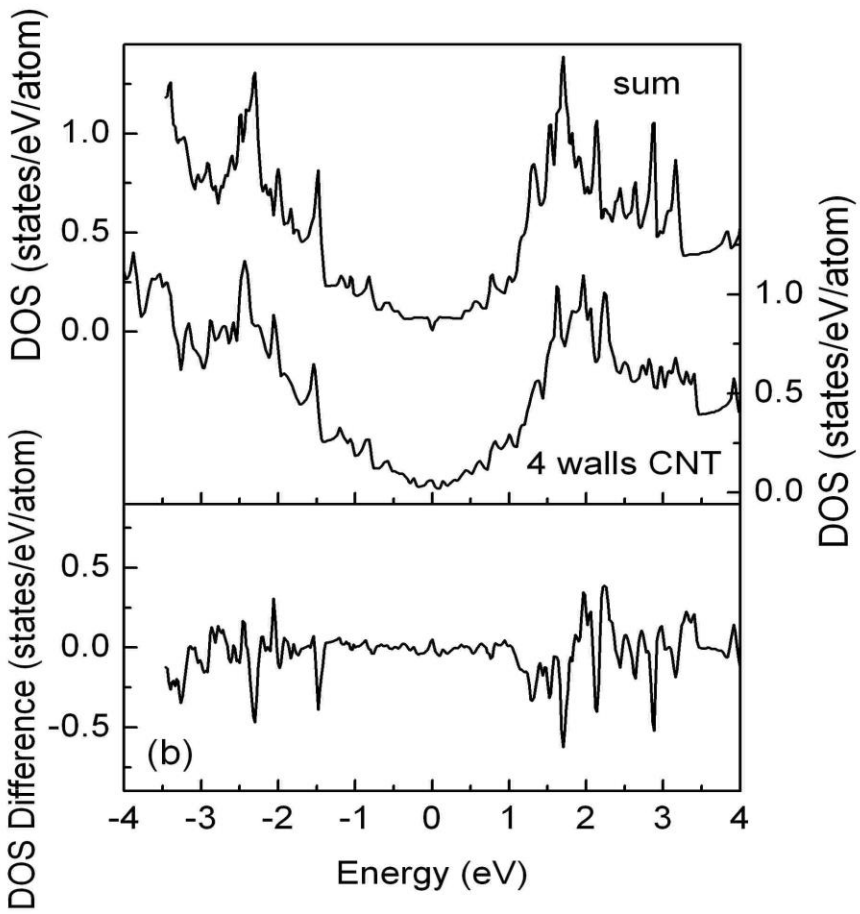

Computation by A.Continenza, L'Aquila University (Italy)
P.Castrucci, M.DeCrescenzi et al., Nanotechnology 22, 115701 (2011)

SWCNT/Si hybrid solar cell

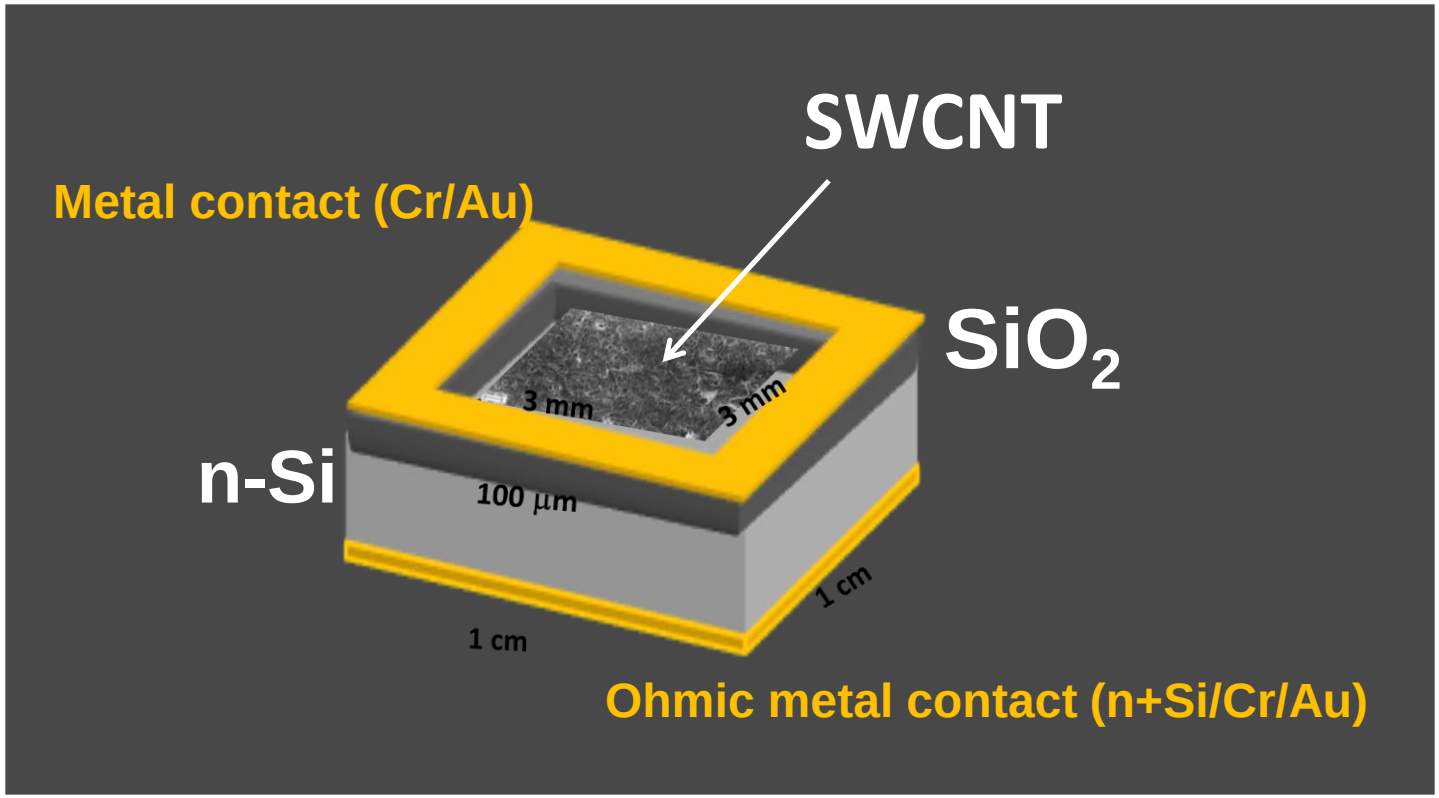

- ☺ **Reduction of the expensive fabrication processes at T ~1000°C and Silicon thickness**
- ☺ **Promising efficiency (11-15%) in laboratory devices**
- ☺ **High stability over time**

CNTs were dispersed in aqueous solution with 2% of sodium-dodecyl-sulfate, ultra-sonicated in ice-bath and the unbundled supernatant was collected by pipette

Carbon nanotube films were fabricated by a vacuum filtration process of the dispersion with mixed cellulose ester filters and can be transferred on any surface

dry transfer printing

F.De Nicola, M.De Crescenzi, P.Castrucci et al. Scientific Reports (2015)

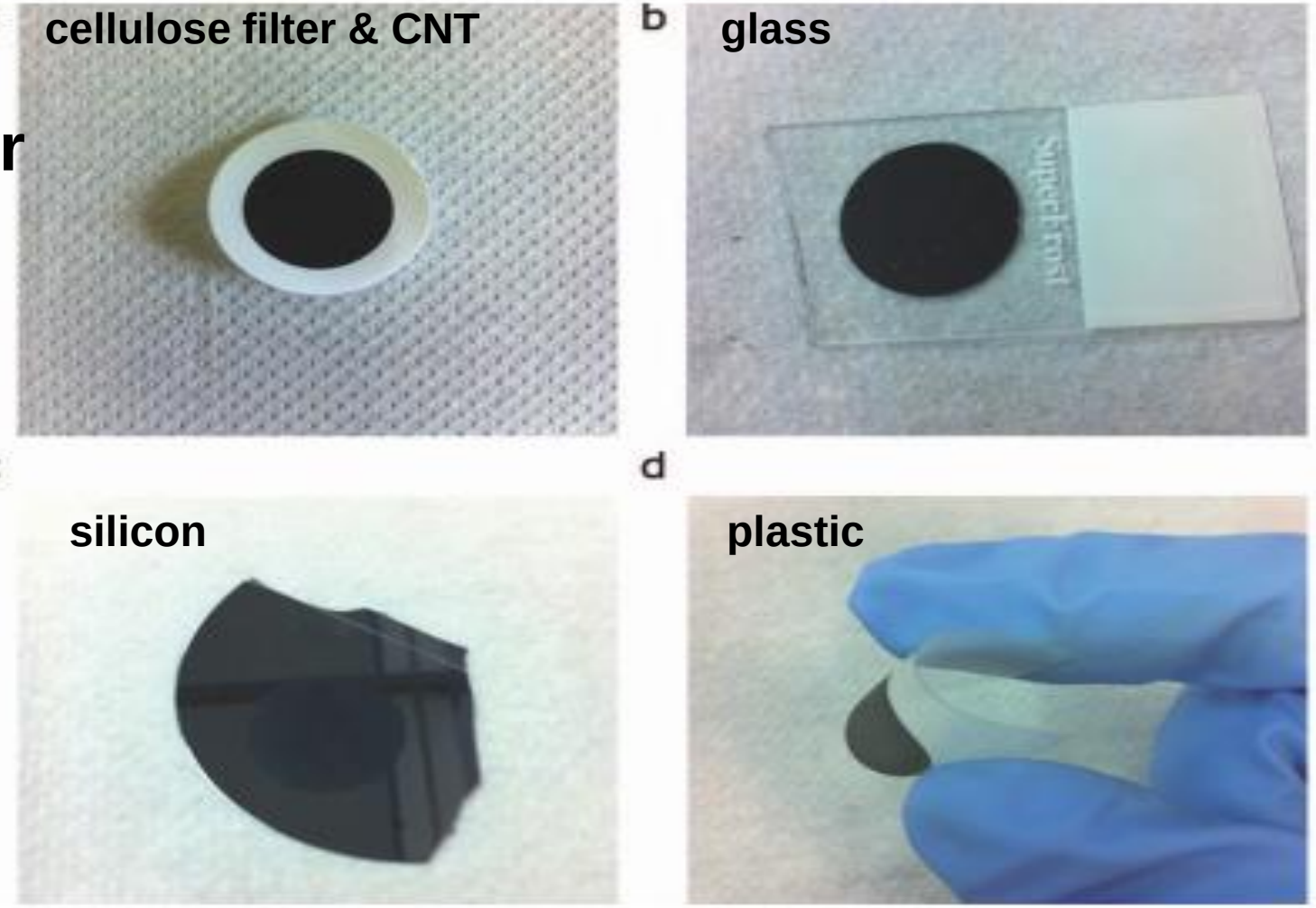

CNT network dry transfer printing

- Aqueous suspension of CNTs and anionic surfactant (SDS)
- Well dispersed suspension (ultrasonication)
- Volume controlled vacuum filtration process on cellulose filter
- Dry-transfer printing deposition method

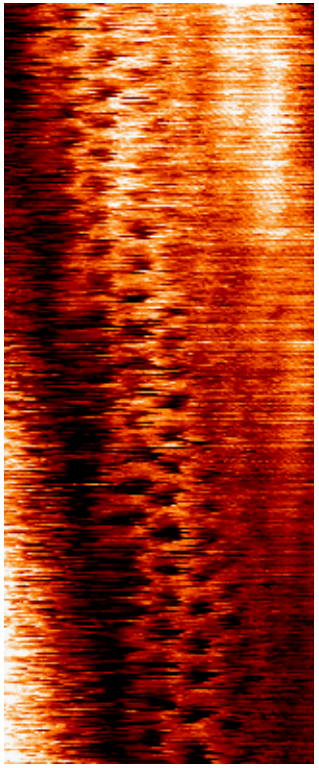

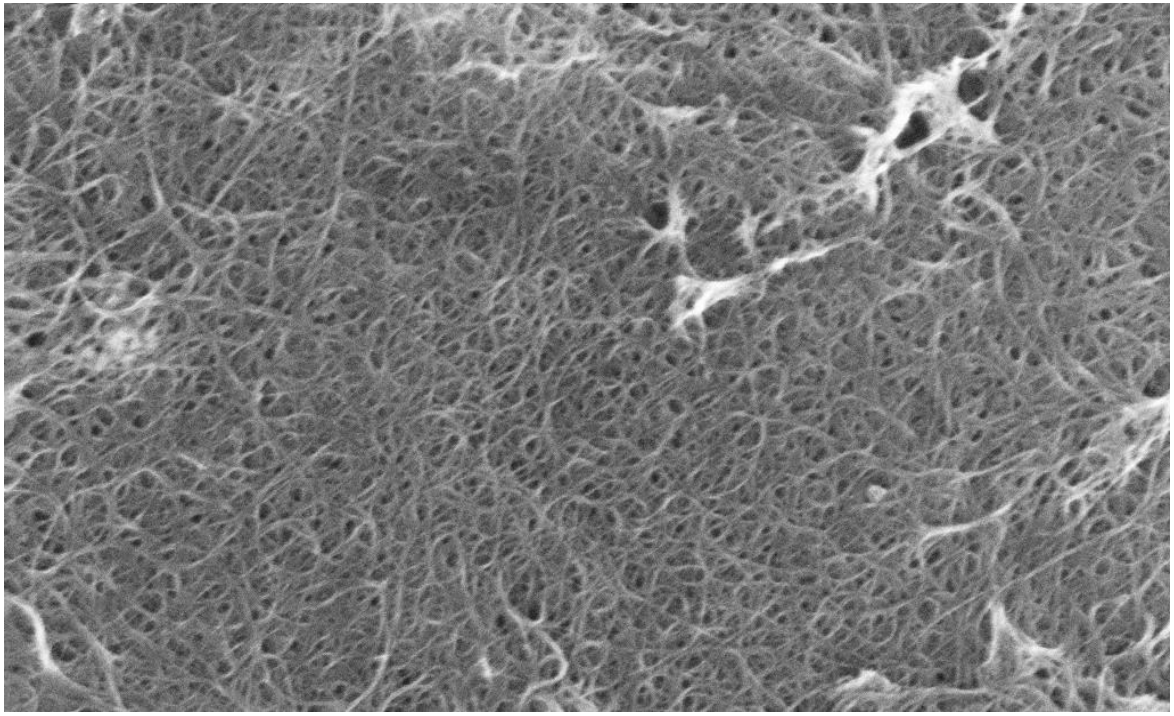

CNT random and porous networks

Low-cost

Rapid

Room-temperature process

Scalable

Highly reproducible

SWCNT network properties

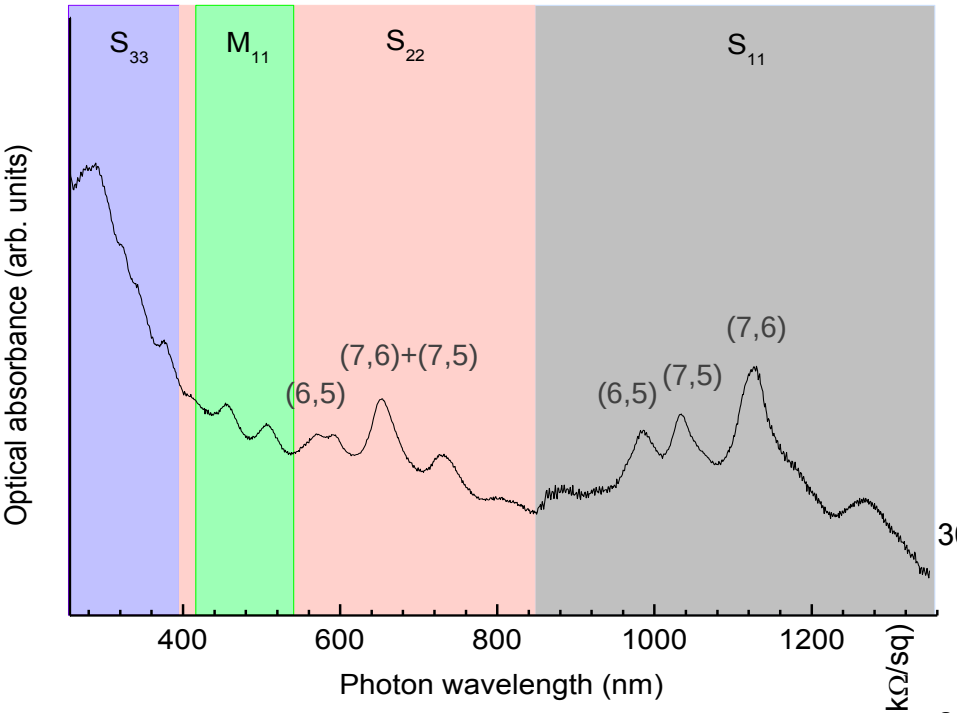

SWCNT diameter: 0.75 - 0.9 nm
85-90% semiconductor SWCNTs
Major chiralities: (7,6), (7,5) and (6,5)

$$T(\lambda) = \left(1 + \frac{Z_0\,\sigma_{ac}(\lambda)}{2\,R_{sh}\sigma_{dc}}\right)^{-2}$$

Z_0 = 377 Ω free space impedence
$\sigma_{ac}(\lambda)$ optical conductivity
σ_{dc} electrical conductivity
$R_{sh} = (\sigma_{dc}\ d)^{-1}$

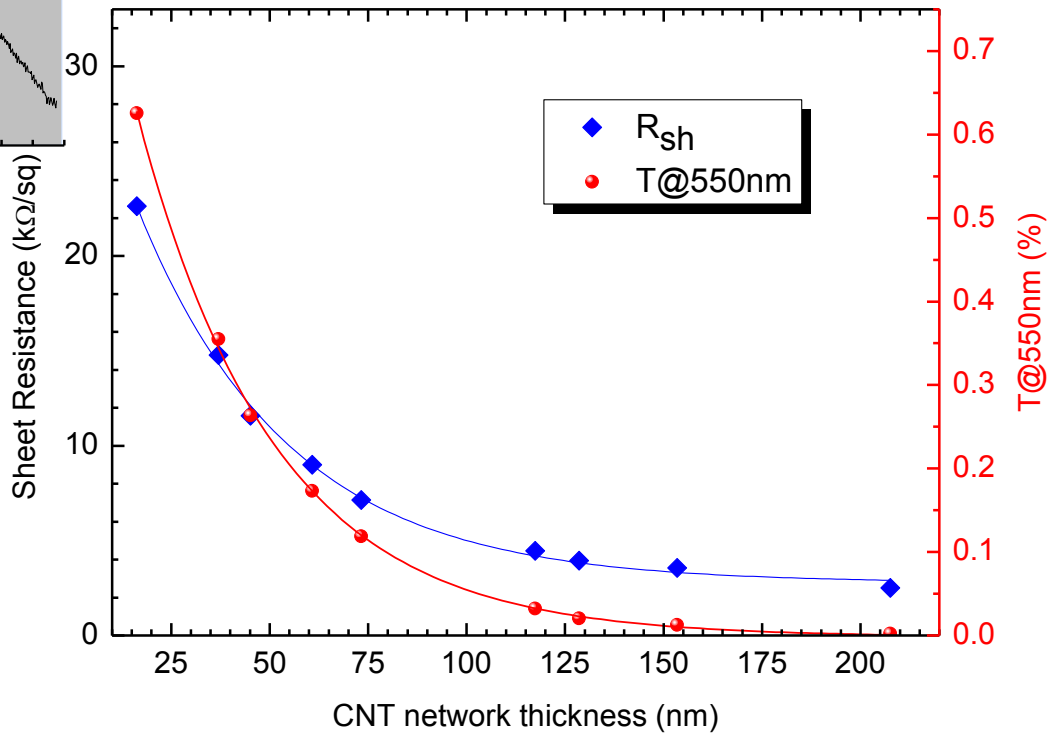

SWCNT/Si hybrid solar cell

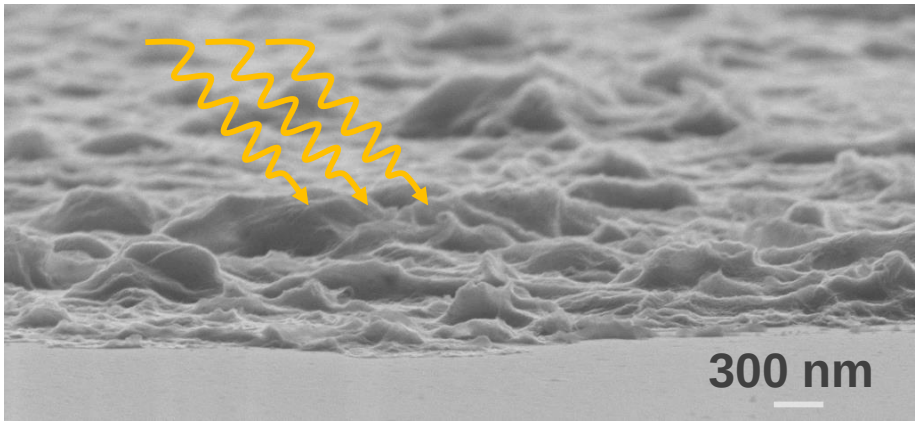

SWCNTs

- **Mostly arranged in small bundle diameter (5-7 nm)**
- **mixed chiralities**

85-90% semiconducting SWCNTs (slightly p-type)

p-n heterojunctions at the SWCNT/n-Si interface

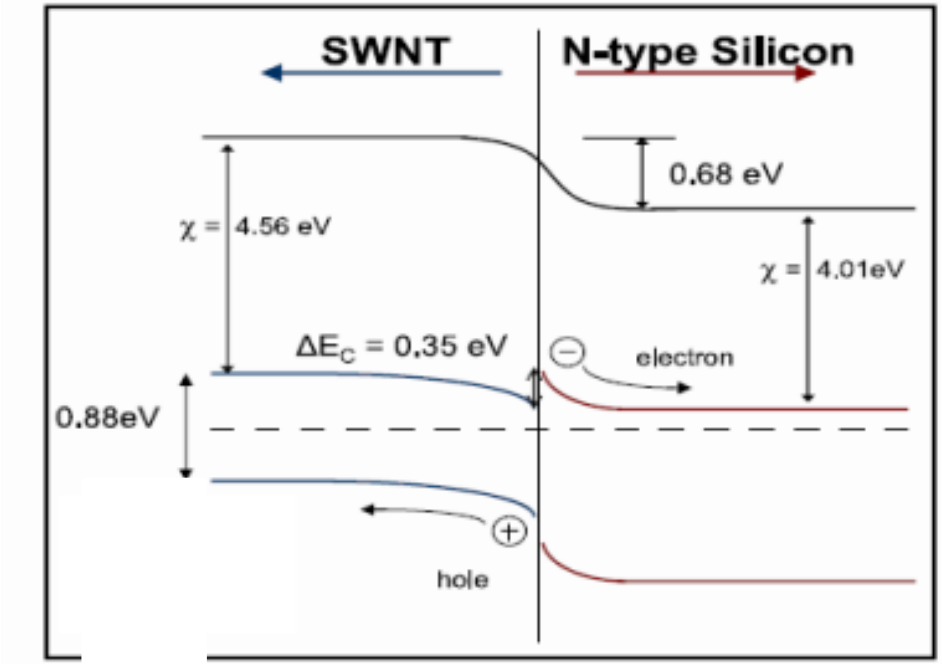

PCE of SWCNT/Si hybrid solar cells

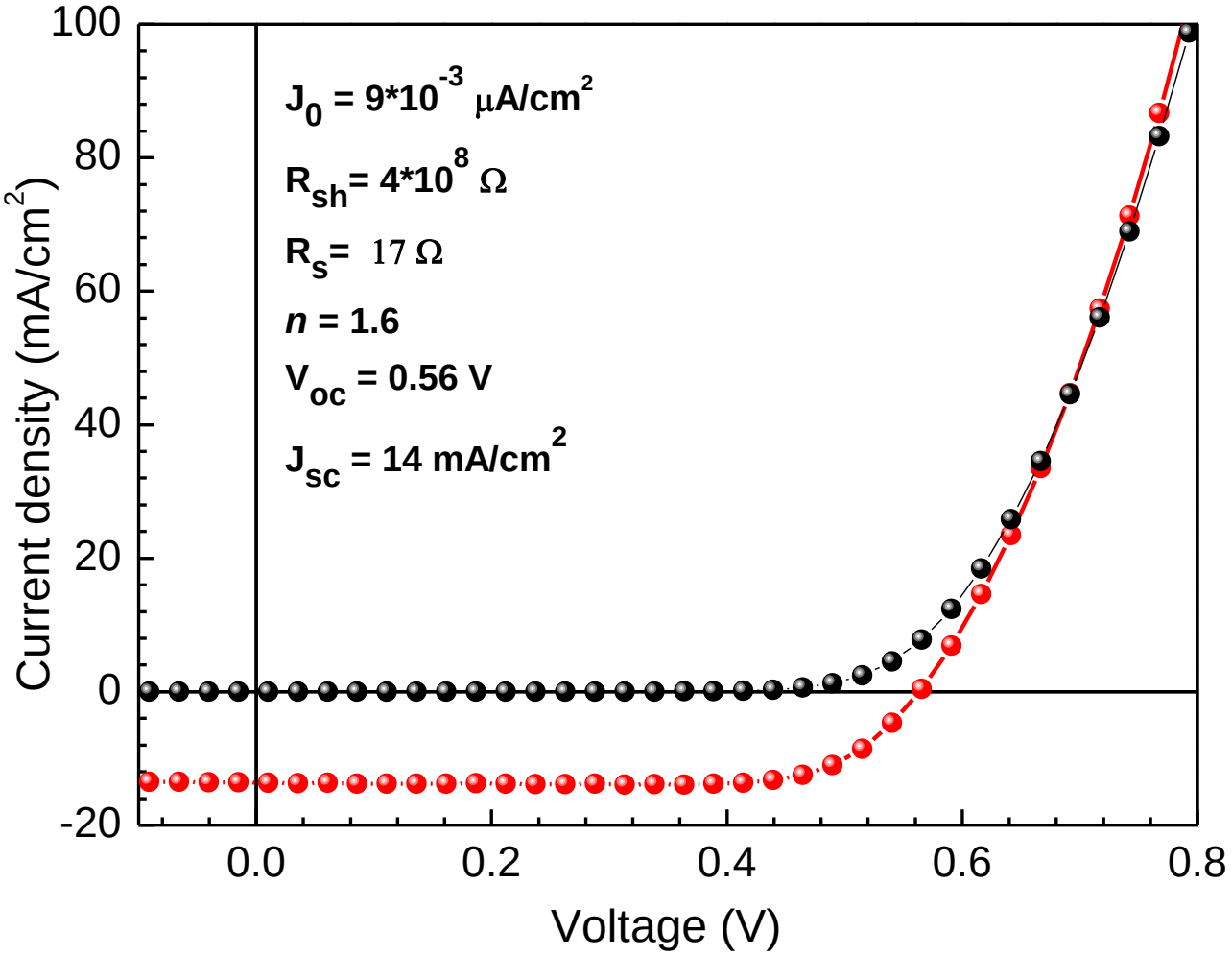

Good performances

Good reproducibility

Good stability over time

AM1.5 Sun Simulator

Del Gobbo, Castrucci, Scarselli, DeCrescenzi et al., J. Mater.Chem. C1, 6752 (2013)

EQE of SWCNT/Si hybrid solar cells

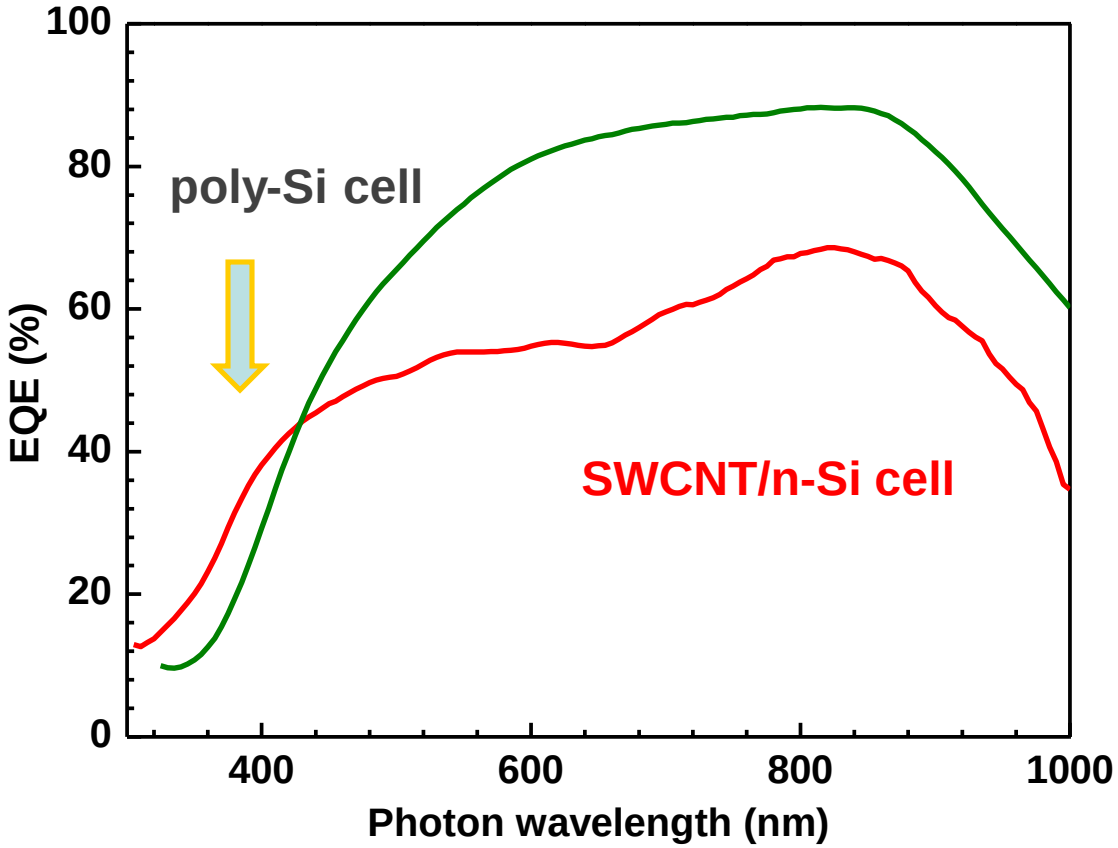

Not too much different!

charge carriers generated into n-Si mainly contribute to photocurrent

EQE extended toward the near UV region

Behaviour vs SWCNT network thickness

The suitable «thickness», d

- Maximize current:
  Lowest R_{sh} => high d
- Maximize e-h pairs from the n-Si base:
  Highest T => low d

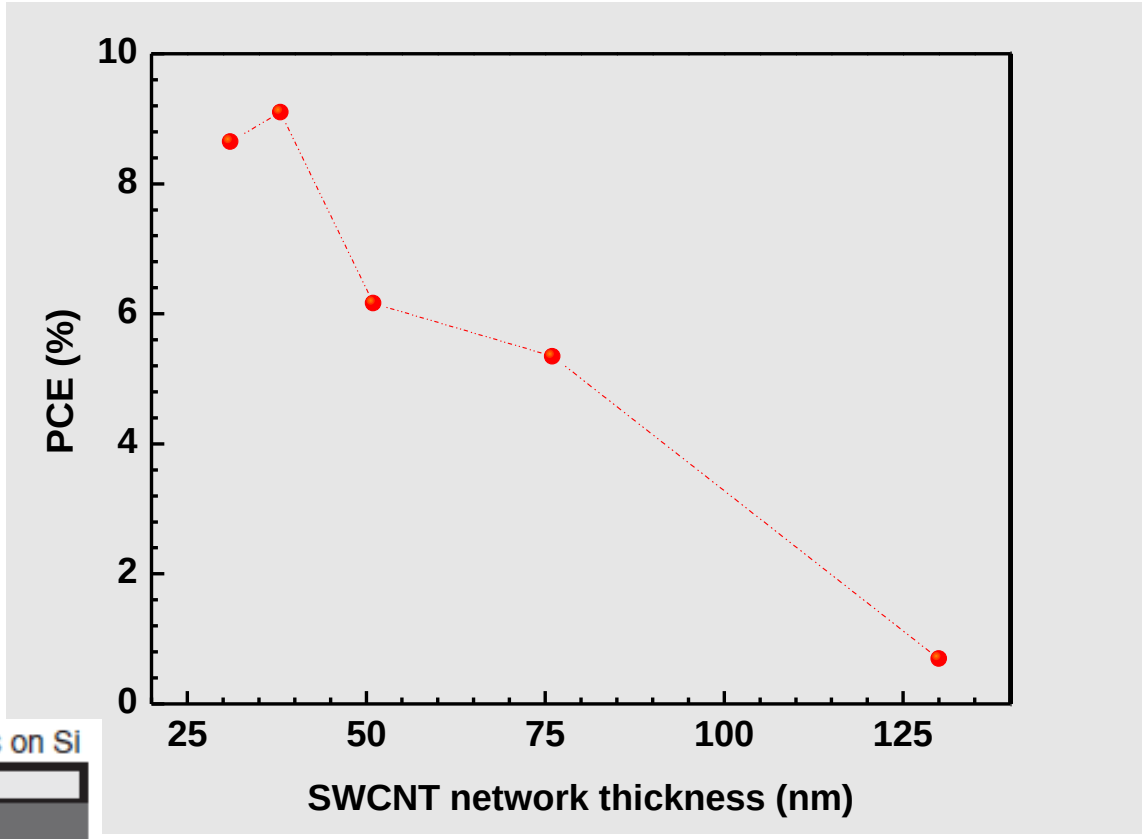

SWCNT network is porous
- empty Si areas
- small CNT bundles
- superposition of CNTs

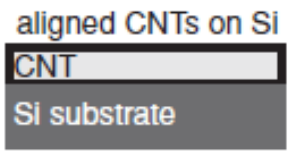

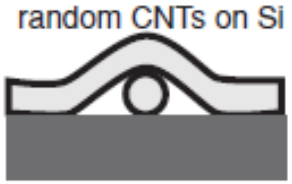

To maximize e-h separation:
Highest number of heterojunctions
=> «right» d

Cell behaviour vs CNT film thickness

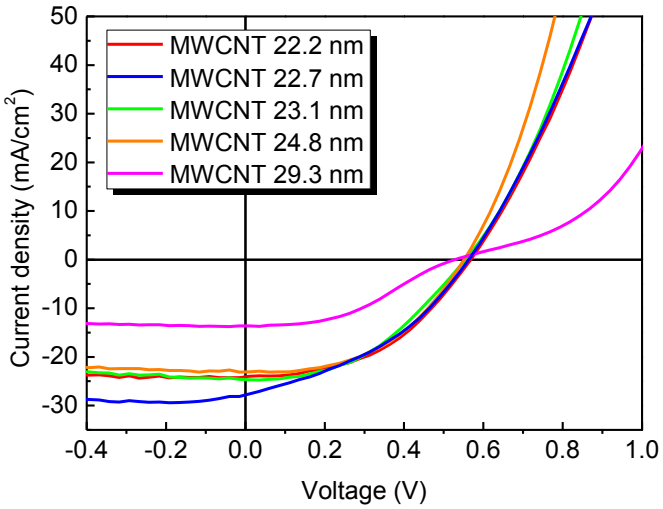

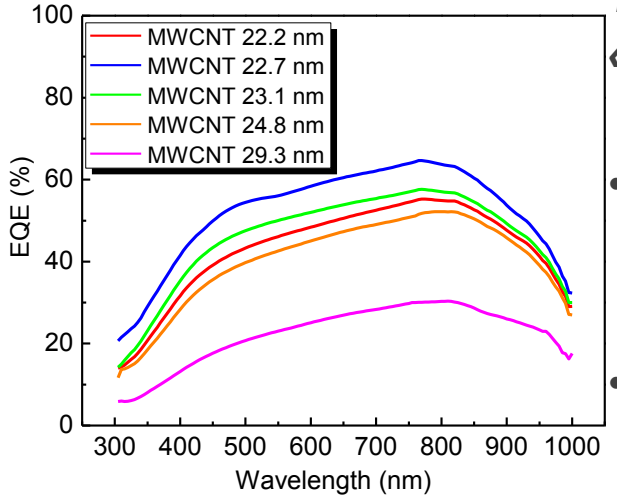

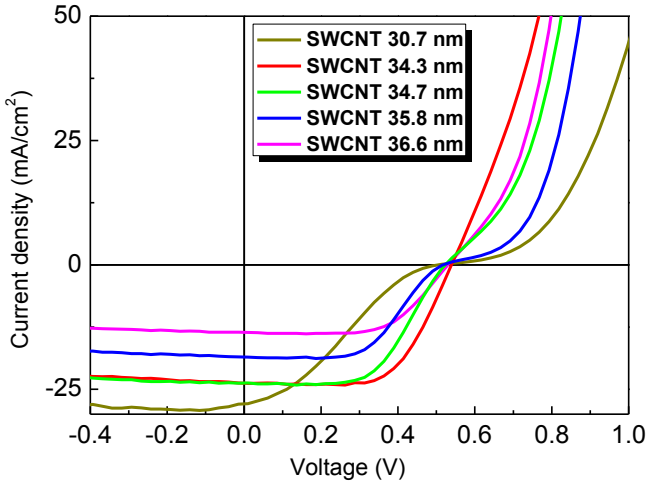

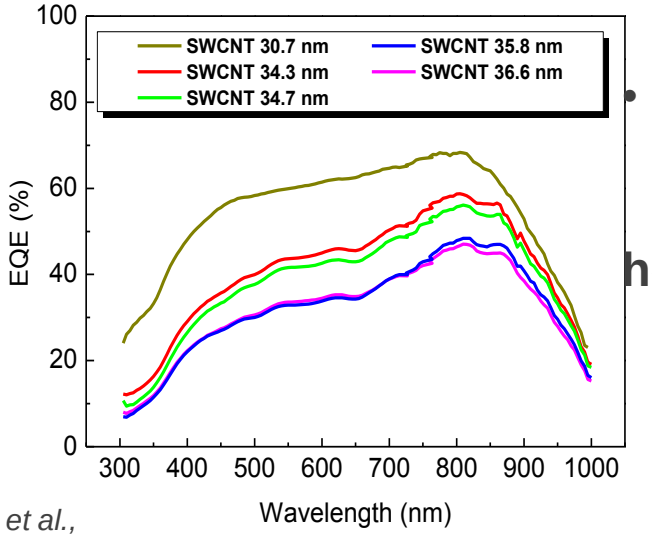

The suitable «thickness», d

- **Maximize current:**
  Lowest R_{sh}
  => *high d*
- **Maximize e-h pairs from the n-Si base:**
  Highest T
  => *low d*
- **Maximize e-h separation:**
  Highest number of heterojunctions
  => *«right» d*

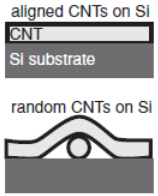

F. De Nicola, M. De Crescenzi, M. Scarselli, P. Castrucci et al., Record efficiency of air-stable multi-walled carbon nanotube/silicon solar cells, Carbon 2016, 101, 226-234.

SWCNT/Si hybrid solar cell stability over time

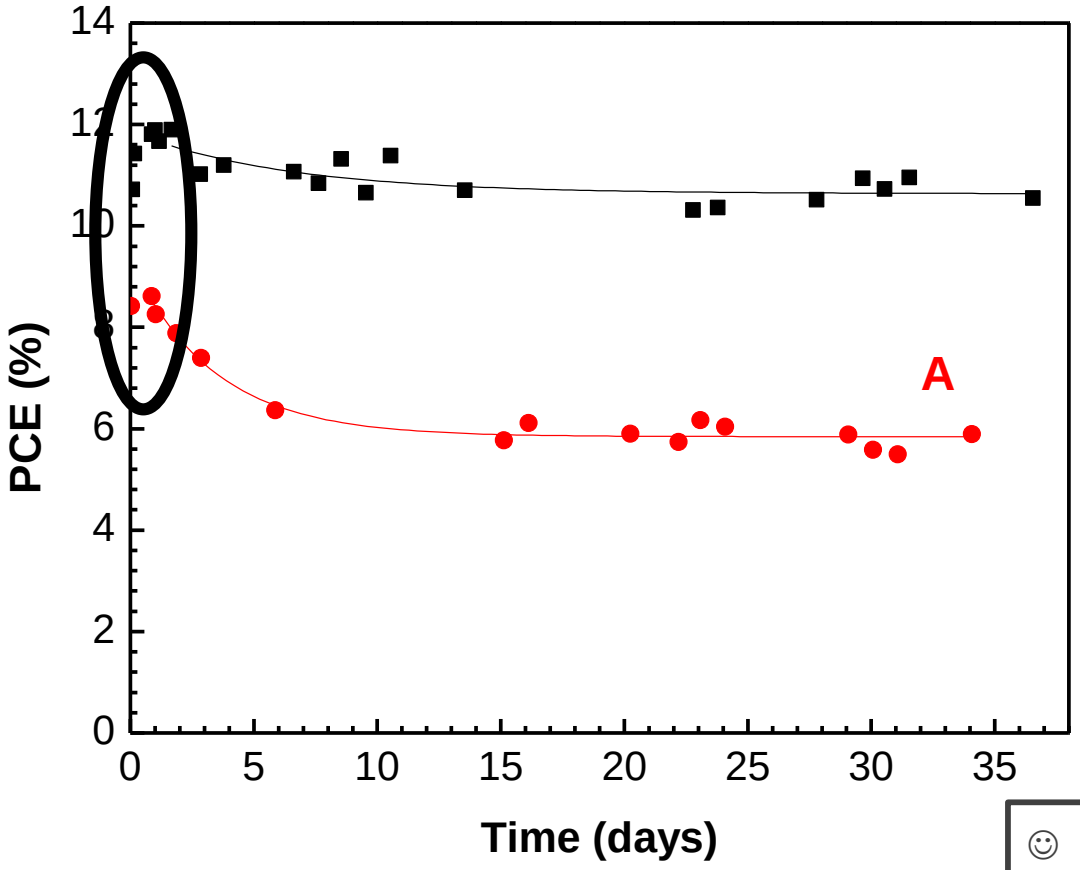

PCE increases in the first 20-24 hours

- **SWCNT network is porous**
- **Bare Si is partially exposed to environmental agents**

☺ **Silicon oxide formation and growth**

☺ **Optimal silicon oxide layer thickness**

XPS and AR-XPS analysis of the oxide layer

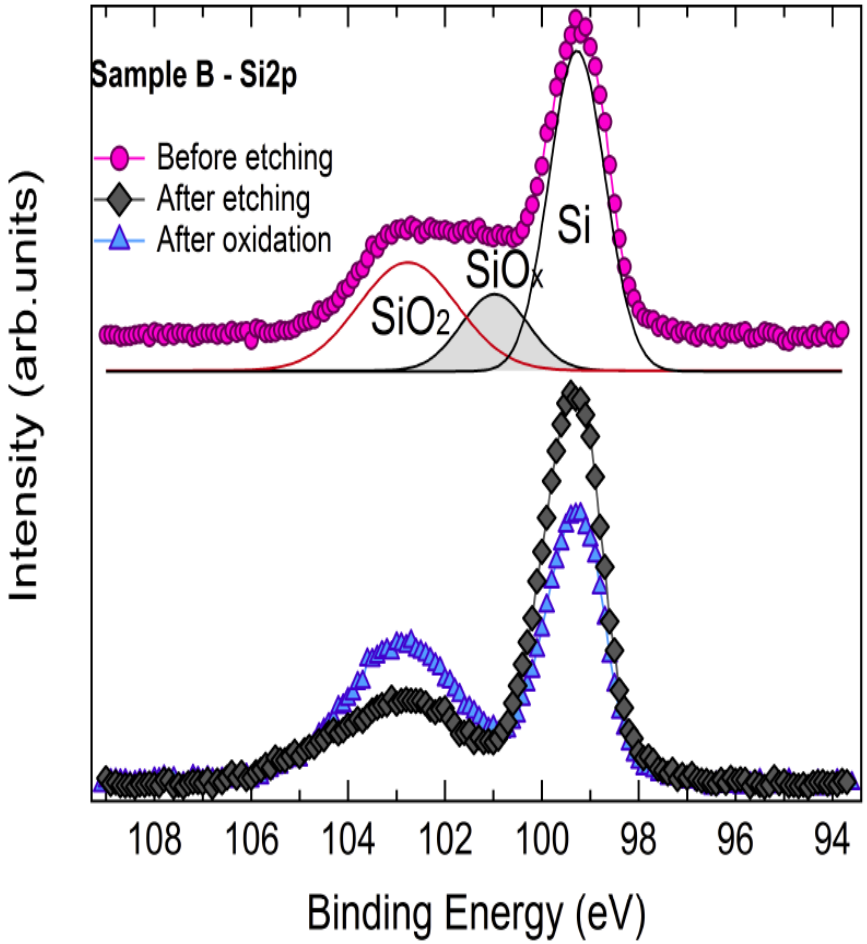

- SiO_2 and SiO_x layers due to silicon oxidation in air
- HF vapor etching reduces the SiO_2 and SiO_x layers
- The optimal thickness of SiO_2 layer is about 1 nm

Pintossi, C., Salvinelli, G., Drera, G., Pagliara, S., Sangaletti, L., Del Gobbo, S., Morbidoni, M., Scarselli, M., De Crescenzi, M., Castrucci, P. J. Phys. Chem. C 117, 18688 (2013)

Beneficial effects of HNO_3 vapours

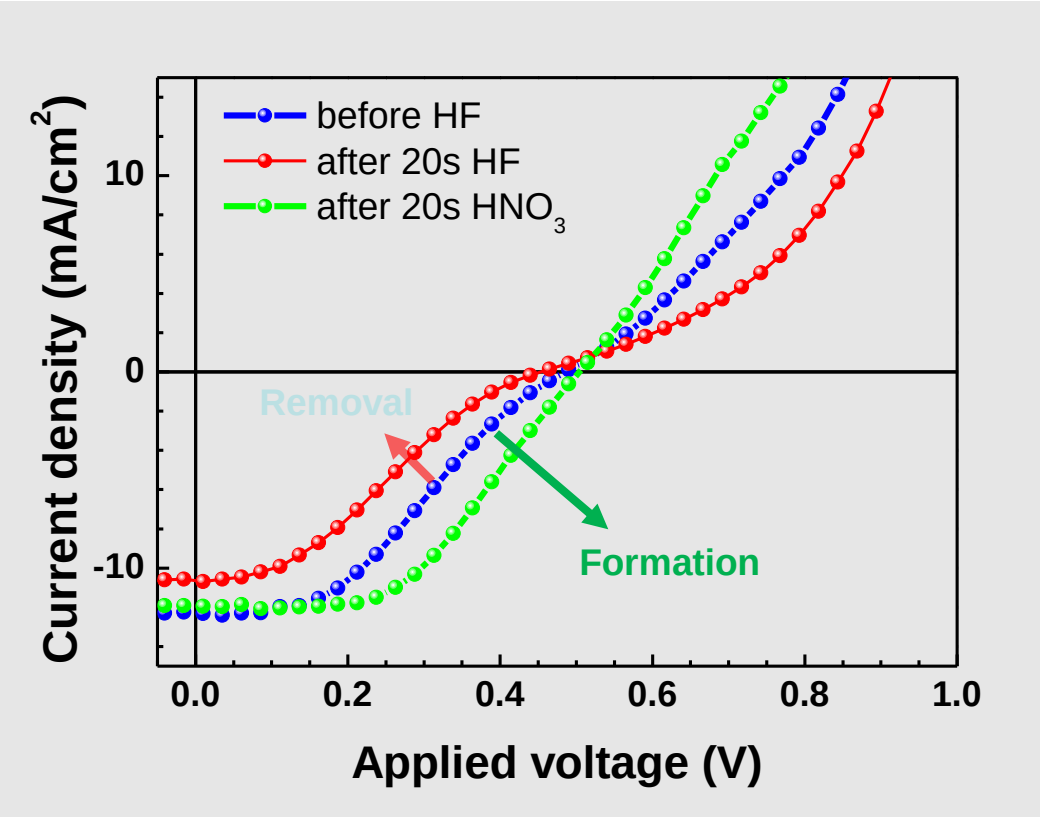

- **HF vapor reduces/removes the silicon oxide layer and provides n-doping**
- **HNO_3 vapors provide the formation of silicon oxide layer and p-doping**

Thin silicon oxide layer gives rise to CNT/Si interface trap-state passivation, thus reducing the recombination effects and improving the ideal diode behaviour of the cell

CNT network properties

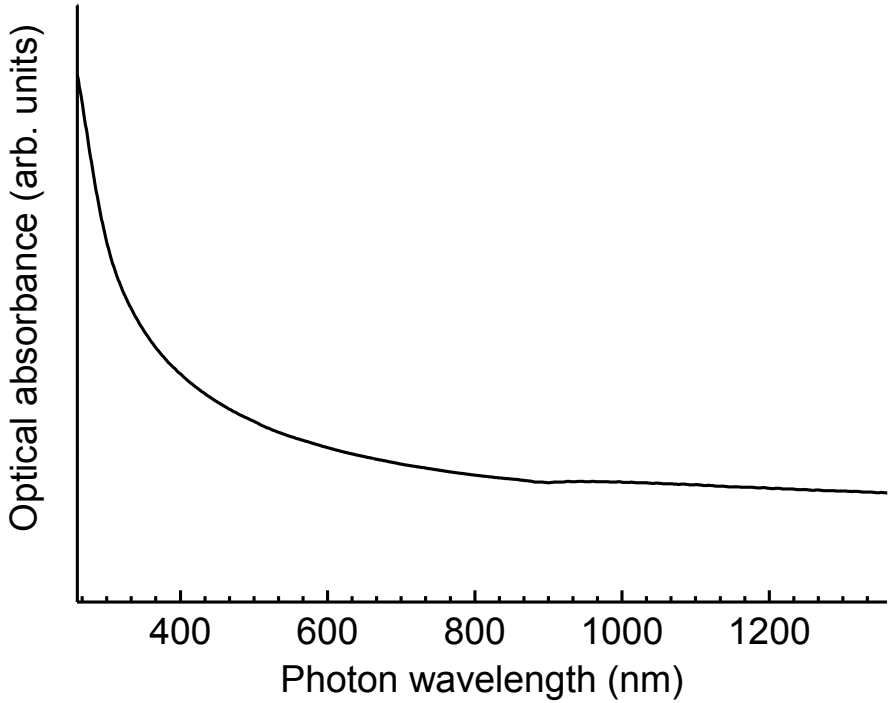

MWCNT average diameter: 9.5 nm

$$T(\lambda) = \left(1 + \frac{Z_0\,\sigma_{ac}(\lambda)}{2\,R_{sh}\sigma_{dc}}\right)^{-2}$$

Z_0 = 377 Ω free space impedence
$\sigma_{ac}(\lambda)$ optical conductivity
σ_{dc} electrical conductivity
$R_{sh} = (\sigma_{dc}\ d)^{-1}$

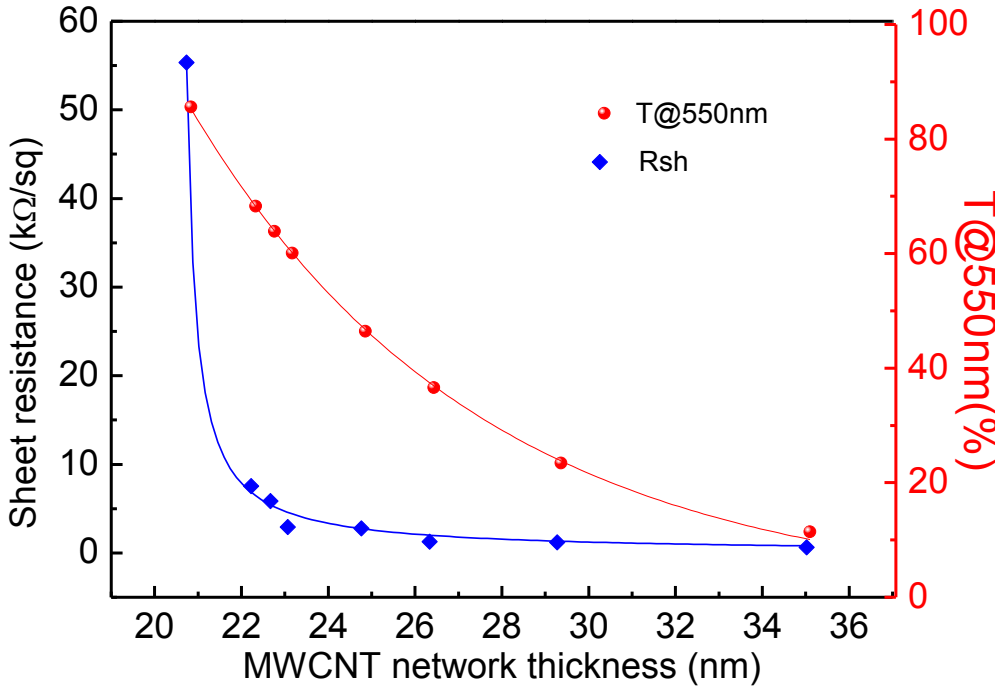

F. De Nicola, S. Pagliara, L. Sangaletti, M. De Crescenzi, P. Castrucci, et al.
Controlling the thickness of carbon nanotube random network films by the estimation of the absorption coefficient, Carbon 2015, 95, 28-33.

PCE of CNT/Si hybrid solar cells

Record performances for MWCNT/Si

(up to now PCE ~ 1-2%)

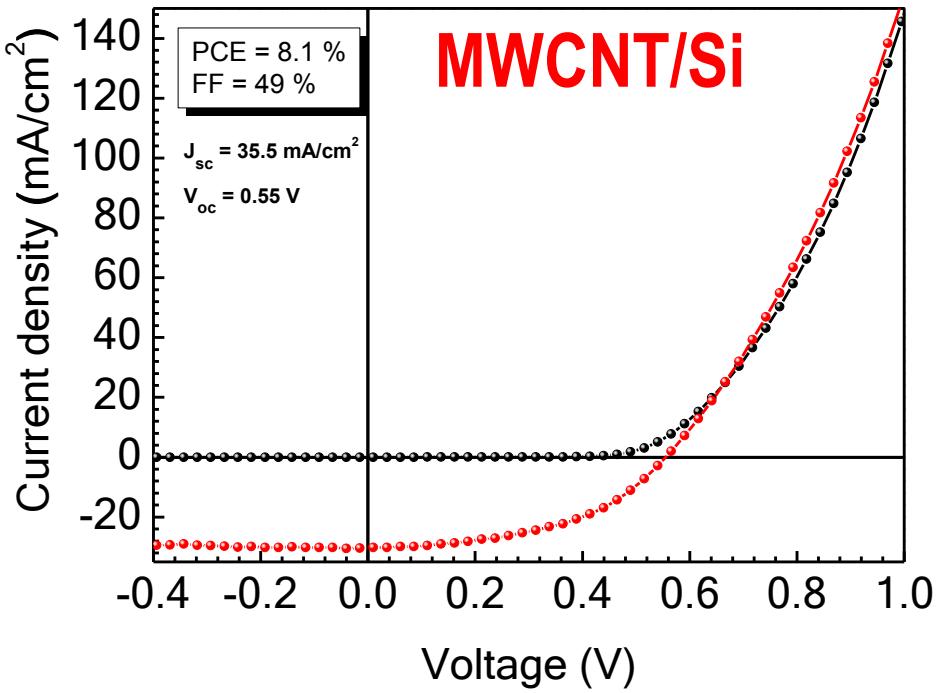

Good reproducibility

Good stability over time

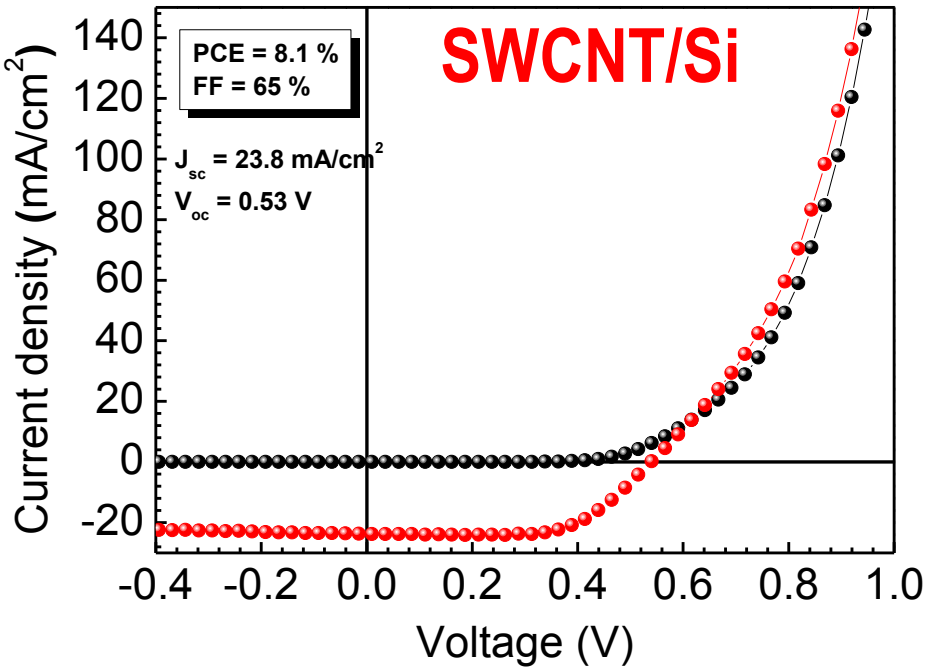

F. De Nicola, M. De Crescenzi, M. Scarselli, P. Castrucci et al., Record efficiency of air-stable multi-walled carbon nanotube/silicon solar cells, Carbon 2016, 101, 226-234.

Beneficial effects of HNO_3 vapour exposure

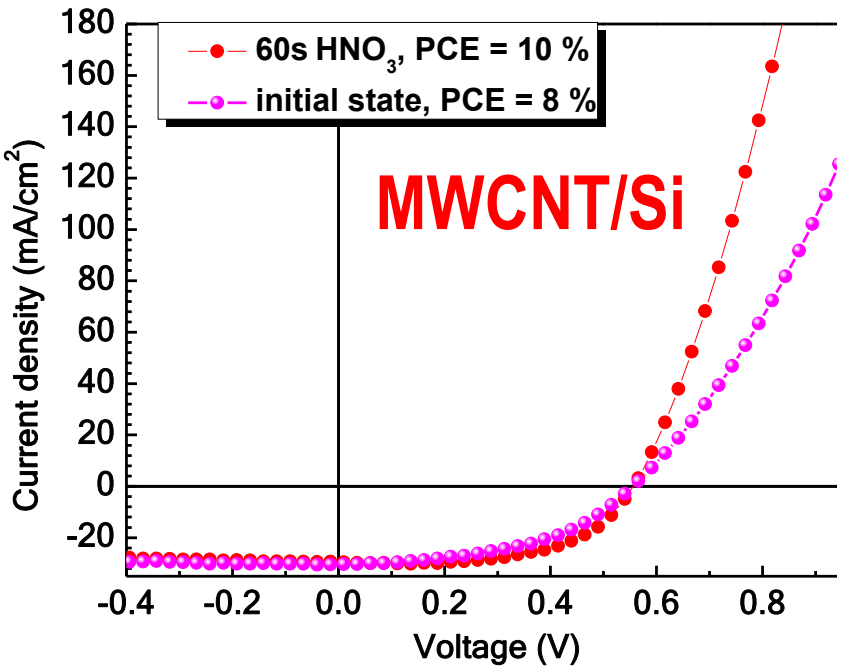

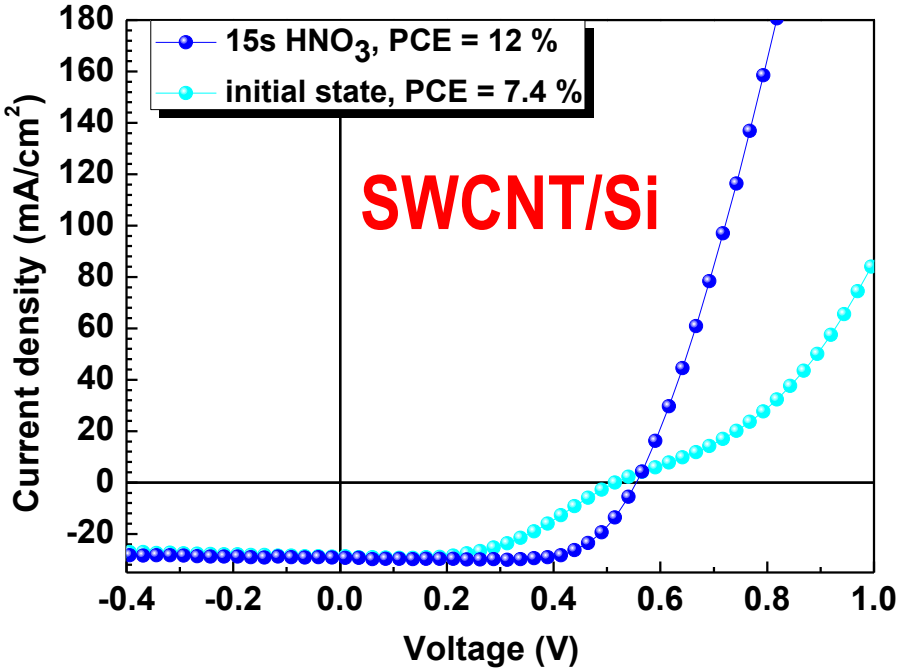

- R_s decreases
- FF increases
- J_{sc} quite constant
- V_{oc} increasing tendency

F. De Nicola, M. De Crescenzi, P. Castrucci et al.,
Record efficiency of air-stable multi-walled carbon nanotube/silicon solar cells, Carbon 2016, 101, 226-234.

The diode characteristics of the Schottky junction could be described by thermionic emission theory[24]

$$J = J_s \left[\exp\left(\frac{eV}{nkT} \right) - 1 \right],$$

where n is the ideality factor, T is the temperature, and J_S is the saturation current density which can be related to the Φ_B expressed as

$$J_s = A^* T^2 \exp\left(-\frac{e\Phi_B}{kT} \right),$$

where A* is the Richardson constant.

Conclusions

- Carbon nanotubes generate photocurrent in the near ultraviolet and visible spectral range (solid state photocurrent measurements and electrochemical cell Graetzel-type). The EQE as well as the I-V efficiency for MWCNTs can reach similar values than that from SWCNTs.

- The photogenerated current depends on several effects: formation of e-h in the CNTs, Schottky barrier with the electrodes, heterojunction formation with substrate. EQE of SWCNTs/Si reached 80%. Crystalline as well as amorphous silicon substrates have been used.

CNT/Si solar cells are very promising

- ☺ Reduction of the Si material and of the expensive fabrication processes at T ~1000°C of conventional Si solar cells, no need of dopants
- ☺ PCE (11-15%), in laboratory devices, comparable to commercial (and optimized) Si solar cells
- ☺ Extension of the EQE of the conventional solar cells toward the near ultraviolet spectral range
- ☺ Stable over time elapsing, without any particular encapsulation
- ☺ Multiple Excitation Generation could enhance the PCE

Collaborations :

P.Castrucci, M.Scarselli, S.Del Gobbo, L.Camilli, F.DeNicola, O.Pulci
(Physics Department, Roma TorVergata, Italy)

M.Venanzi, E.Gatto (Chem. Dept., Roma TorVergata, Italy)
Photo-electrochemical current measurements

M. Crivellari, M. Boscardin
Bruno Kessler Foundation, Povo, Italy
Crystalline n-Si devices

C. Pintossi, S. Pagliara, L. Sangaletti
Dipartimento di Fisica, Università del Sacro Cuore di Brescia, Brescia, Italy
XPS measurements and simulation

M. Passacantando, V. Grossi
Dipartimento di Fisica, Università dell'Aquila, Italy,
Cross-section SEM

V.Le Borgne, M.A.El Khakani
(Université du Québec,Varennes, Canada)
SWCNTs by laser deposition

High Efficiency Carrier Multiplication in PbSe Nanocrystals: Implications for Solar Energy Conversion

R. D. Schaller and V. I. Klimov

Chemistry Division, C-PCS, Los Alamos National Laboratory, Los Alamos, New Mexico 87545, USA

(Received 25 November 2003; published 5 May 2004)

We demonstrate for the first time that impact ionization (II) (the inverse of Auger recombination) occurs with very high efficiency in semiconductor nanocrystals (NCs). Interband optical excitation of PbSe NCs at low pump intensities, for which less than one exciton is initially generated per NC on average, results in the formation of two or more excitons (carrier multiplication) when pump photon energies are more than 3 times the NC band gap energy. The generation of multiexcitons from a single photon absorption event is observed to take place on an ultrafast (picosecond) time scale and occurs with up to 100% efficiency depending upon the excess energy of the absorbed photon. Efficient II in NCs can be used to considerably increase the power conversion efficiency of NC-based solar cells.

Enhanced photovoltaic efficiency by impact ionization (inverse Auger)

A.J.Nozik, Physica E14, 115 (2002)

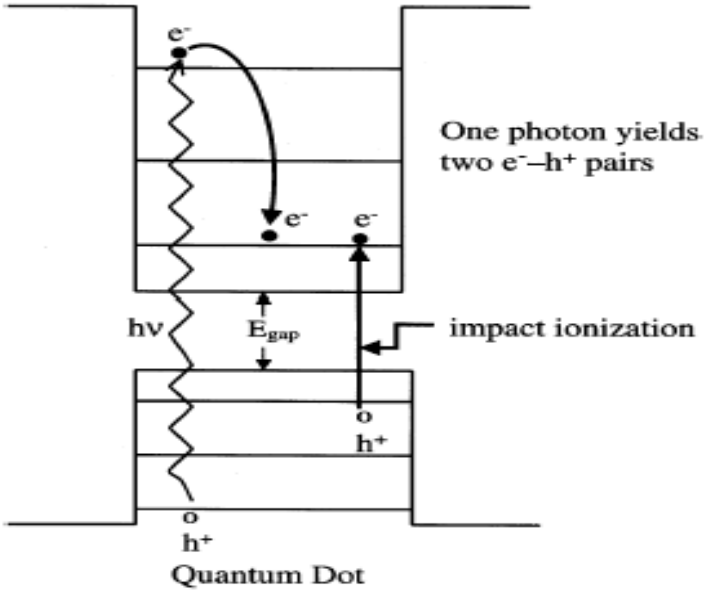

Beneficial effects of HNO_3 vapour exposure

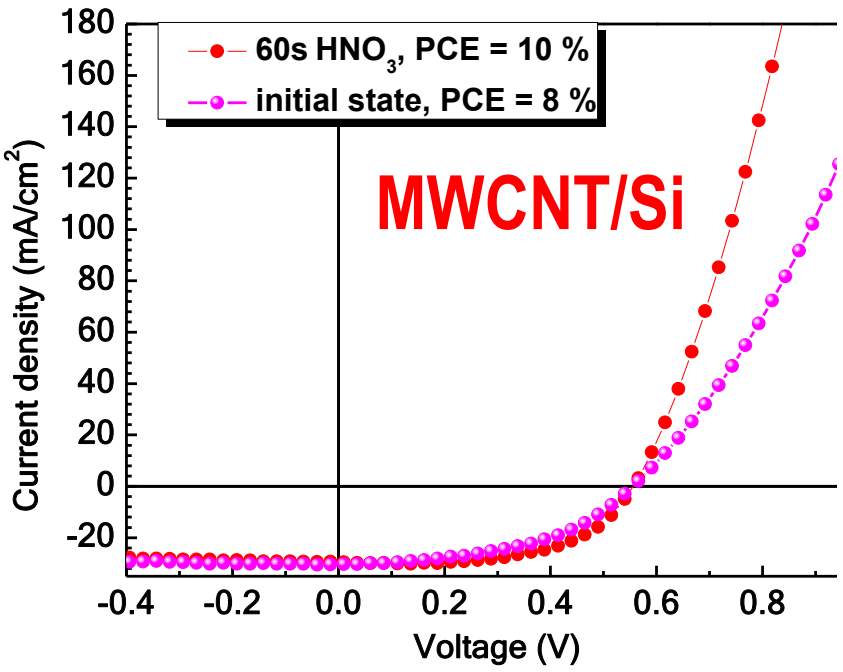

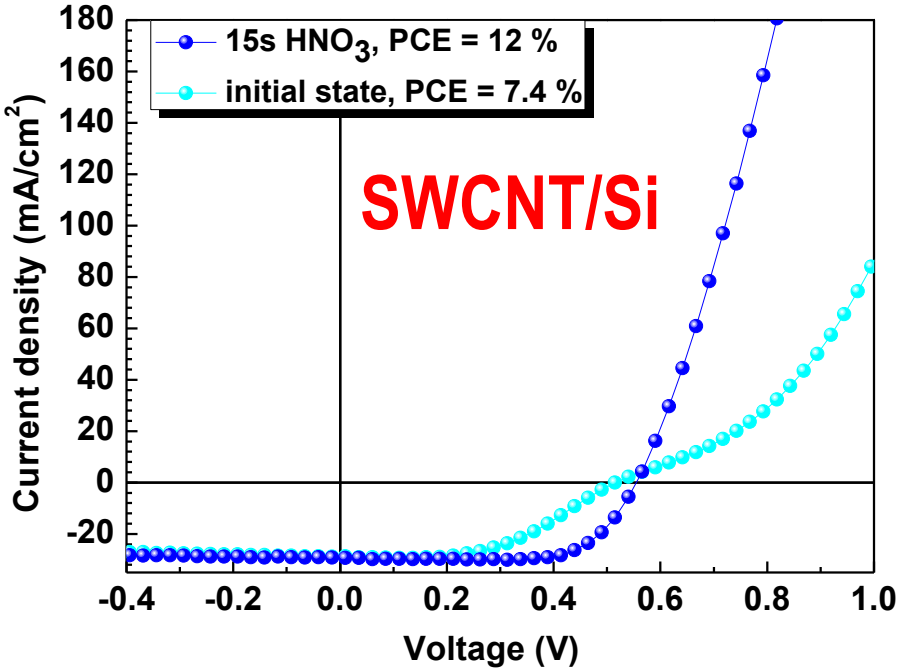

- R_s decreases
- FF increases
- J_{sc} quite constant
- V_{oc} increasing tendency

F. De Nicola, M. De Crescenzi, P. Castrucci et al.,
Record efficiency of air-stable multi-walled carbon nanotube/silicon solar cells, Carbon 2016, 101, 226-234.

Beneficial effects of HNO_3 vapour exposure

- HF vapor reduces/removes the silicon oxide layer and provides low n-doping
- HNO_3 vapor provides the formation of “suitable” silicon oxide layer (quite stable) and p-doping

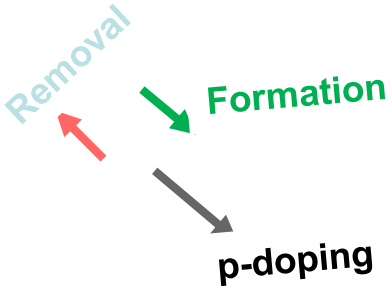

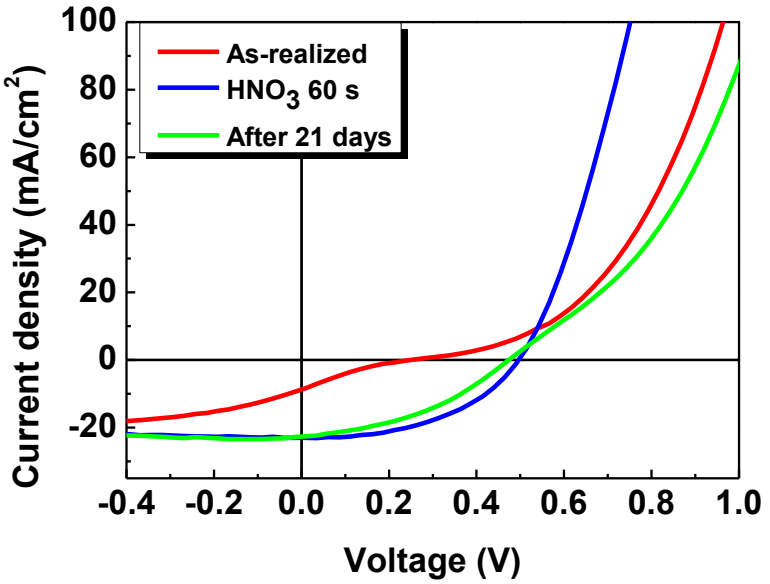

- Thin silicon oxide layer gives rise to CNT/Si interface trap-states, thus reducing the recombination effects and improving the ideal diode behaviour of the cell

F. De Nicola, M. De Crescenzi, M. Scarselli, P. Castrucci et al., Record efficiency of air-stable multi-walled carbon nanotube/silicon solar cells, Carbon 2016, 101, 226-234.

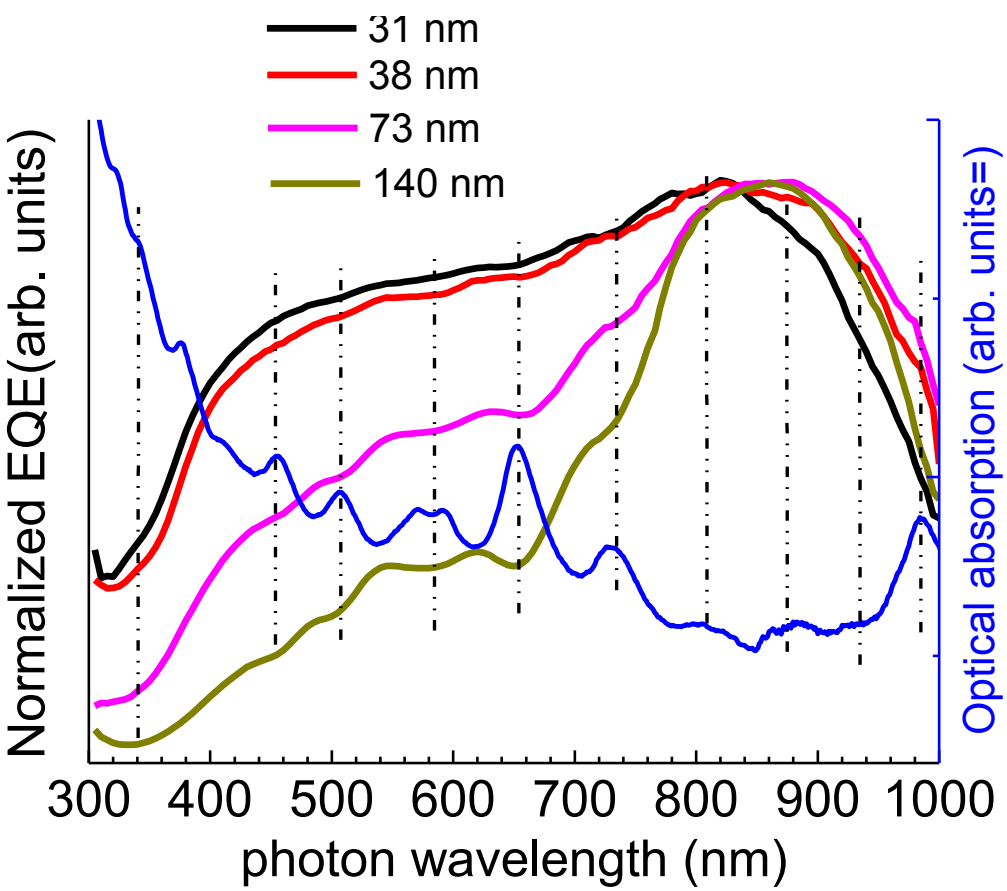
31 nm
38 nm
73 nm
140 nm
Normalized EQE(arb. units)
Optical absorption (arb. units=)
300 400 500 600 700 800 900 1000
photon wavelength (nm)

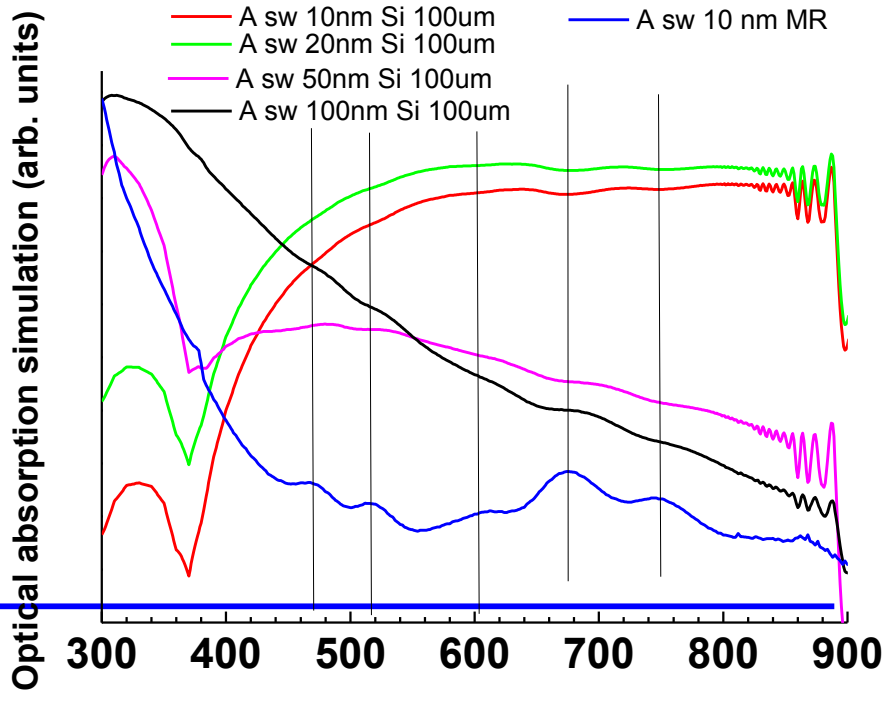
A sw 10nm Si 100um
A sw 20nm Si 100um
A sw 50nm Si 100um
A sw 100nm Si 100um
A sw 10 nm MR
Optical absorption simulation (arb. units)
300 400 500 600 700 800 900

Behaviour vs SWCNT network thickness

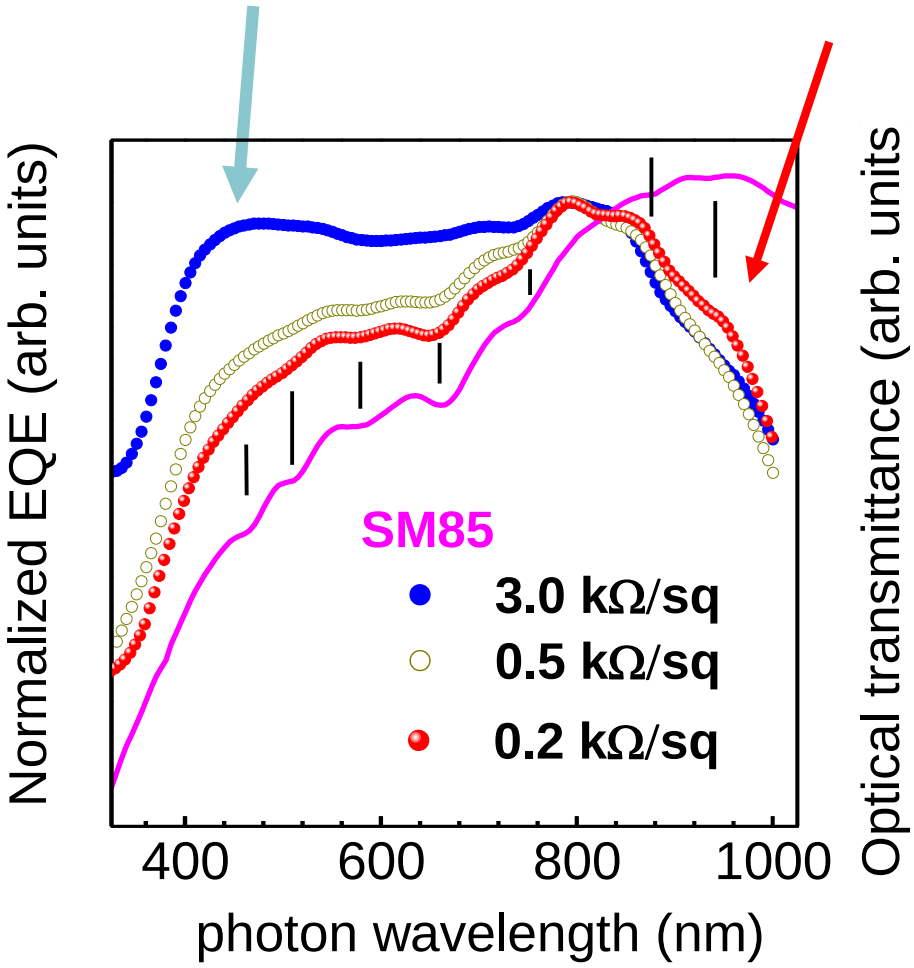

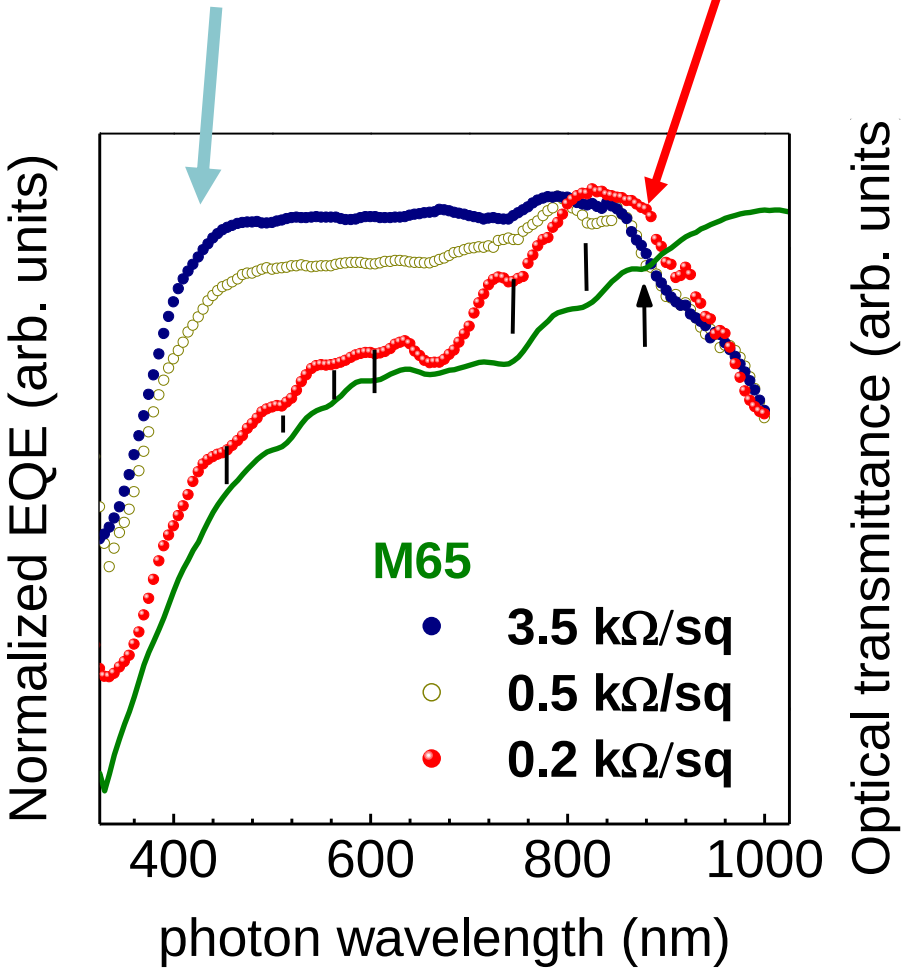

- **SWCNTs contribute to photocurrent**
- **Metal SWCNTs contribute to photocurrent**
- **Si spectral range extention toward the near UV and the near IR region**

Del Gobbo, S. Castrucci, P., Fedele, S., Riele, L., Convertino, A., Morbidoni, M., De Nicola, F., Scarselli, M., Camilli, L., De Crescenzi, M. (2013), Journal of Mater. Chemistry C, DOI: 10.1039/c3tc31038h

HNO_3 and HF vapour exposure

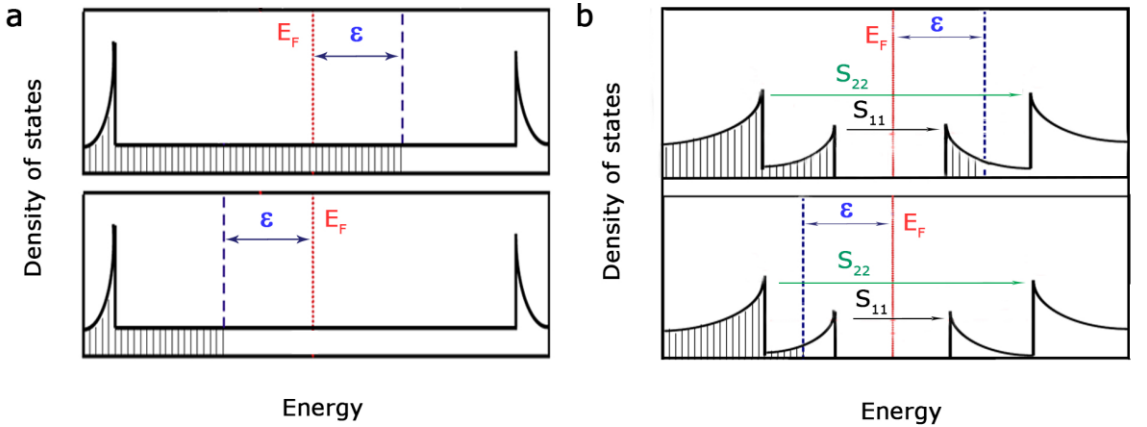

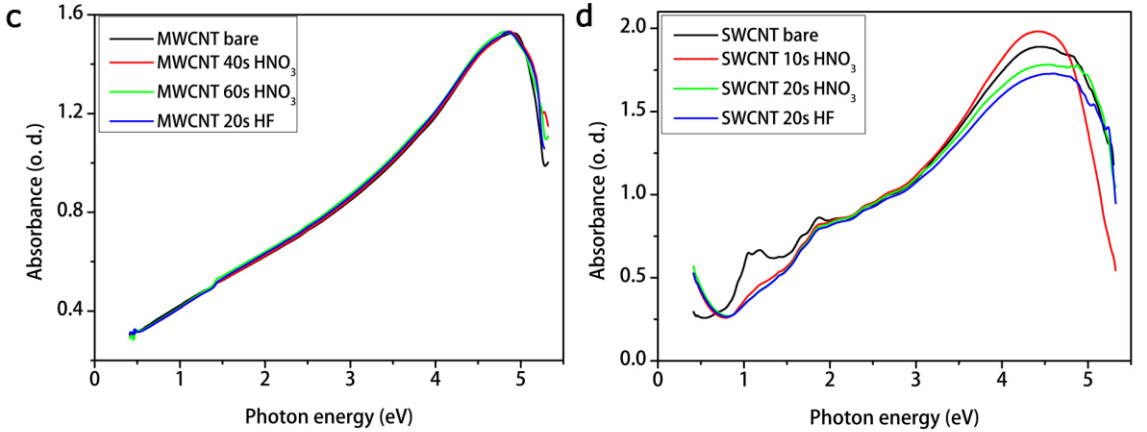

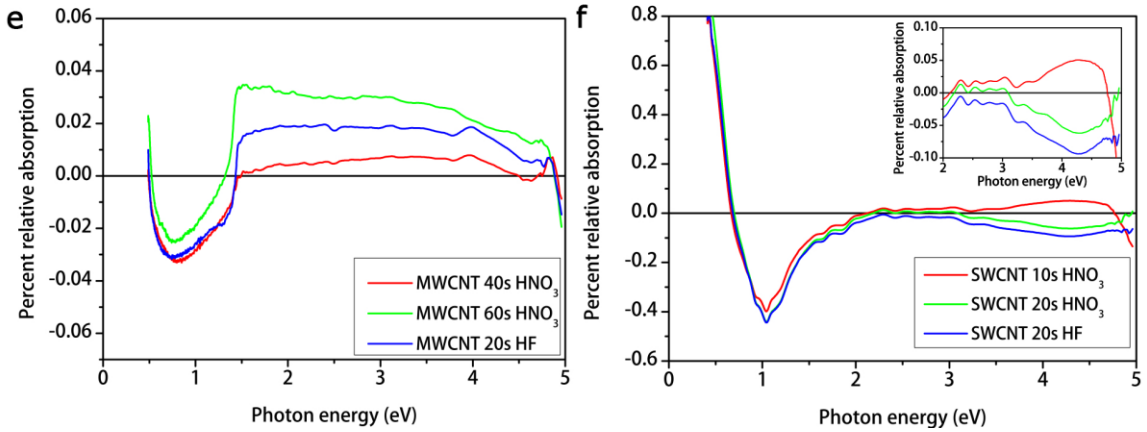

Upon HNO_3 exposure

- **Free carriers increase in MWCNT and metallic SWCNT -> NIR absorption increase**
- **Less available states in the near UV-Vis region due to the higher energy shift of the Fermi level ->**
  - **--- partial bleaching of the S_{11} and S_{22} transitions in SWCNT case**
  - **--- overall reduction of optical absorption in this region**

MWCNT/Si **SWCNT/Si**

SWCNT/Si

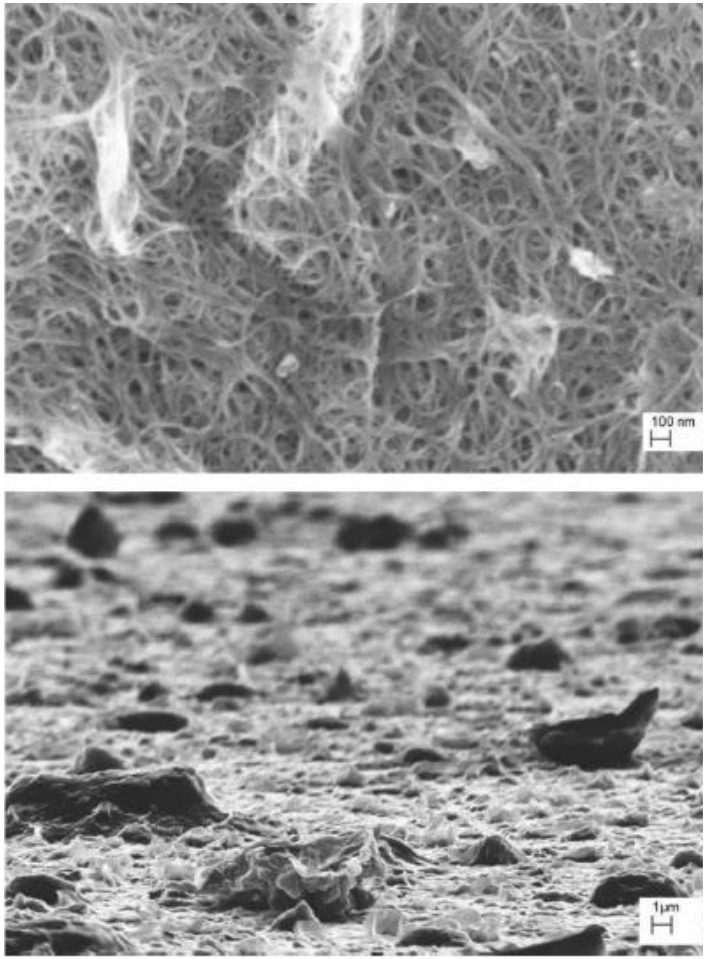

MWCNT/Si

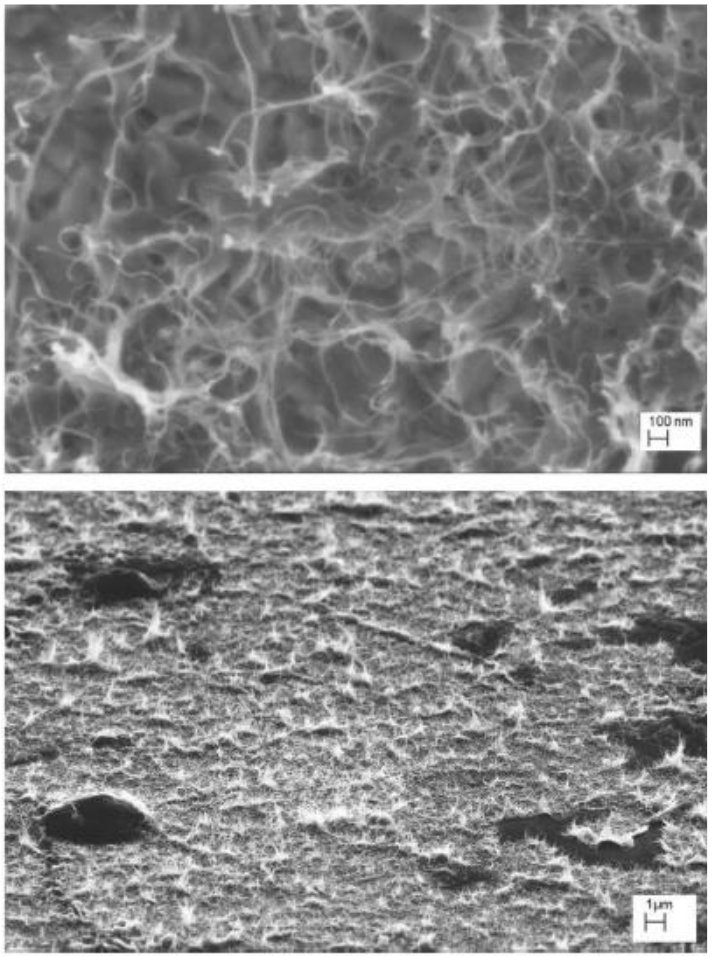

sample	ρ (nm)	*d* (nm)	*S* (µm^2)	*h* (µm)
SWCNT	2–8	4–8	0.003–0.007	1.6–11.7
MWCNT	40–44	34–84	—	—

UNIVERSITÀ DI ROMA TOR VERGATA

F. De Nicola, P. Castrucci, M. Scarselli, M. De Crescenzi et al., Beilstein J. Nanotechnol. 2015, 6, 353-360